Temporal evolution, petrography and composition of dolostones in the Upper Devonian Plavinas Regional Stage, southern Estonia and northern Latvia

Anne Kleesment[a], Kristjan Urtson[a], Tarmo Kiipli[a], Tõnu Martma[a], Anne Põldvere[b], Toivo Kallaste[a], Alla Shogenova[a] and Kazbulat Shogenov[a]

[a] Institute of Geology at Tallinn University of Technology, Ehitajate tee 5, 19086 Tallinn, Estonia; kleesmen@gi.ee, urtson@gi.ee, tarmo.kiipli@gi.ee, Tonu.Martma@gi.ee, alla@gi.ee, shogenov@gi.ee
[b] Tartu Regional Department, Geological Survey of Estonia, Rõõmu tee 1, 51013 Tartu, Estonia; anai@ut.ee

Received 19 June 2012, accepted 9 November 2012

Abstract. The Upper Devonian Plavinas Regional Stage in southern Estonia and northern Latvia is represented by dolostones containing interlayers of dolomitic marlstones and limestones. Petrographic, cathodoluminescence, electron microprobe and isotope techniques were used to investigate diagenetic evolution of dolostones. The rock succession has been affected by multiple diagenetic events. Based on petrographic and geochemical data, six dolomite textures were identified. The crystal size (5–1200 μm) and morphology of dolomites are variable. Commonly, dolomites are close to the stoichiometric composition, with low iron and manganese content. Their stable isotope composition ($\delta^{13}C$, $\delta^{18}O$) differs greatly from that of dolomite precipitated from Frasnian seawater. Dolomitization is more pronounced in the lower part of the studied sequence, in the Snetnaya Gora Formation and Lower Pskov unit where carbonates are completely dolomitized, whereas upwards in the section the dolomite content decreases. Voids and pores of the Lower Pskov unit are mainly open, but partly or completely occluded in the Upper Pskov unit. Void-filling dolomite has slightly and void-filling calcite notably depleted stable isotope signatures. Major dedolomitization and calcite-filling processes took place during the final uplift and emergence of the northern part of the Baltic basin, connected with the migration of karst-related meteoric waters into previously dolomitized horizons within carbonate rocks.

Key words: carbonate rocks, diagenesis, dolomite types, stable isotopes, Devonian, Baltic basin.

INTRODUCTION

The uppermost part of the Devonian sequence in southern Estonia and northern Latvia is composed of carbonate rocks representing mainly the Plavinas Regional Stage (RS), exposed as a narrow belt extending from West Latvia to the southern bank of Lake Pskov (Fig. 1; Sorokin 1978). The major part of the section is dolomitized. Petrographically and geochemically the dolostones of the Plavinas RS differ significantly from Early–Middle Devonian early diagenetic dolostones (Kleesment & Shogenova 2005; Kleesment 2007; Shogenova et al. 2007; Tänavsuu-Milkeviciene et al. 2009; Kleesment et al. 2012). It is suggested (Stinkulis 1998, 2008) that main diagenetic alterations in Plavinas rocks took place in already lithified rocks, however, these have not been studied in detail as yet. The diagenetic history of Devonian platform carbonates in other regions has been investigated by Dix (1993), Drivet & Mountjoy (1997), Qing (1998), Potma et al. (2001), Fu et al. (2006), Luczaj et al. (2006), and Vandeginste et al. (2009).

Numerous studies concern dolostones of different diagenetic evolution and ages, whereas various dolomitization models have been proposed (Read 1985; Hardie 1987; Mazzullo 1994; Conioglio et al. 2003; Machel 2004; Lavoie et al. 2005). To explain massive early diagenetic dolomitization of platform carbonates associated with evaporates, Fu et al. (2006) applied the hypersaline brine model. For dolostones, not obviously related to evaporates, the brackish-water mixing zone model (Hardie 1987; Kyser et al. 2002; Azmy et al. 2009) has been considered appropriate. Diffusion of magnesium from seawater is thought to be the most important process for dolomitization (Potma et al. 2001; Machel 2004). The dolostones that formed in different diagenetic environments can be recognized by differences in their petrography, spatial distribution, and geochemical and isotopic signatures, which developed in varying fluid-driving mechanisms, temperature and chemical composition of the dolomitizing fluids (Machel & Mountjou 1986; Qing 1998; Lonnee & Al-Aasm 2000; Green & Mountjoy 2005; Jones 2005). Dolostones may re-equilibrate many times

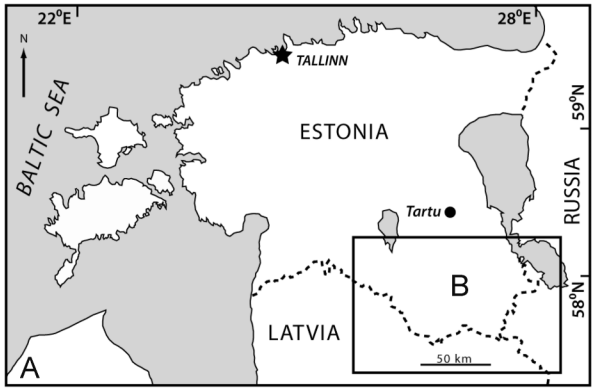

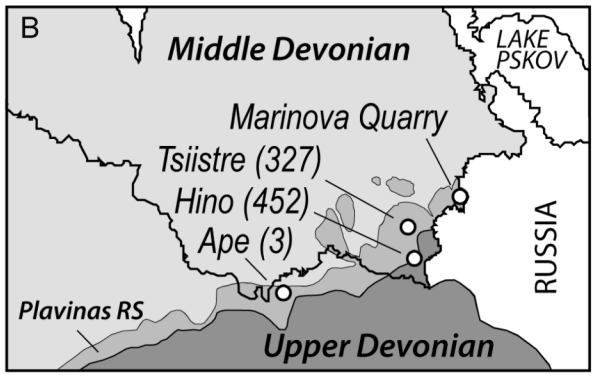

Series	Stage	Regional Stage	Formation	Main lithology
UPPER DEVONIAN	Frasnian	Dubniki		Dolostone
		Plavinas	Chudovo	
			Pskov	
			Snetnaya Gora	
		Amata	Amata	Sandstone
	?	Gauja	Gauja	
MIDDLE DEVONIAN	Givetian	Burtnieki	Burtnieki	Sandstone

Fig. 1. (**A**) Location of the study area and (**B**) distribution of the rocks of the Plavinas RS with locations of the studied sections. The outcrop area of the Plavinas RS after Sorokin (1978) and Suuroja (1997). The stratigraphical scheme of the Middle–Upper Devonian boundary beds of Estonia and Latvia modified after Kleesment et al. (2012) and Mark-Kurik & Põldvere (2012).

during their burial history (Warren 2000; Rifai et al. 2006; Machel & Buschkuehle 2008). Large, replacive dolostone bodies are post-depositional and formed during some degree of burial, which includes effects of sedimentary loading, tectonic compression and pressure solution (Coniglio et al. 2003).

The present study is focused on dolomitization processes of the Plavinas RS, providing novel data on the isotopic composition and cathodoluminescence properties. The characteristics of texturally different dolomite types are described and their diagenetic history is interpreted.

GEOLOGICAL SETTING

The study area lies in southeastern Estonia and northern Latvia, representing the northwestern part of the shallow epicontinental sea (Sorokin 1978). Here, after the regression of the Middle Devonian Baltic basin at the end of Amata time, a transgression of Frasnian age started from the Moscow Syneclise that expanded from shallow epicontinental sea (Nikishin et al. 1996).

Carbonate rocks of the Plavinas Age accumulated during transgression in a normal salinity basin, which was connected to the open sea in the Moscow Syneclise. These carbonate rocks formed during the maximum transgression of sea in Early Frasnian time and are rich in fauna (brachiopods, pelecypods, gastropods, cephalaspods, corals, stromatoporoids, stromatolites, oncoids and fishes; Sorokin 1978; Stinkulis 1998). After deposition and lithification the rocks were affected by a variety of diagenetic processes, including dolomitization and recrystallization.

The 27–32 m thick section of the Plavinas RS is represented by dolostones with interlayers of dolomitic marlstones and limestones (Sorokin 1978; Kajak 1997; Kleesment 2007). It lies on the siliciclastic complex of the Amata Formation (Fm) and is covered by gypsum-containing carbonate rocks of the Dubniki Fm (Sorokin 1978). The Plavinas RS is divided into the Snetnaya Gora, Pskov and Chudovo formations (Fms) (Fig. 1), which have been described by several authors (Sorokin 1978; Kajak 1997; Stinkulis 1998; Mark-Kurik & Põldvere 2012).

Dolostones of the Plavinas RS have often high porosity (Sorokin 1978). Besides porosity related to dolomitization, some porosity is produced by meteoric waters flowing through the rocks and causing karstification (Bishoff et al. 1994; Cunningham et al. 2009). Karst dissolution processes in the Plavinas carbonate rocks have been active since the end of the Late Devonian to the present day (Paukstys & Narbutas 1996; Satkunas et al. 2007).

MATERIAL AND METHODS

We studied in detail the Upper Devonian sequences in the Tsiistre (327), Hino (452) (SE Estonia) and Ape (3) (NE Latvia) drill cores and in Marinova quarry (SE Estonia) (Figs 1, 2). A total of 63 rock samples were collected. Thirty-two thin sections were examined under a polarizing microscope. Five thin sections were examined using a

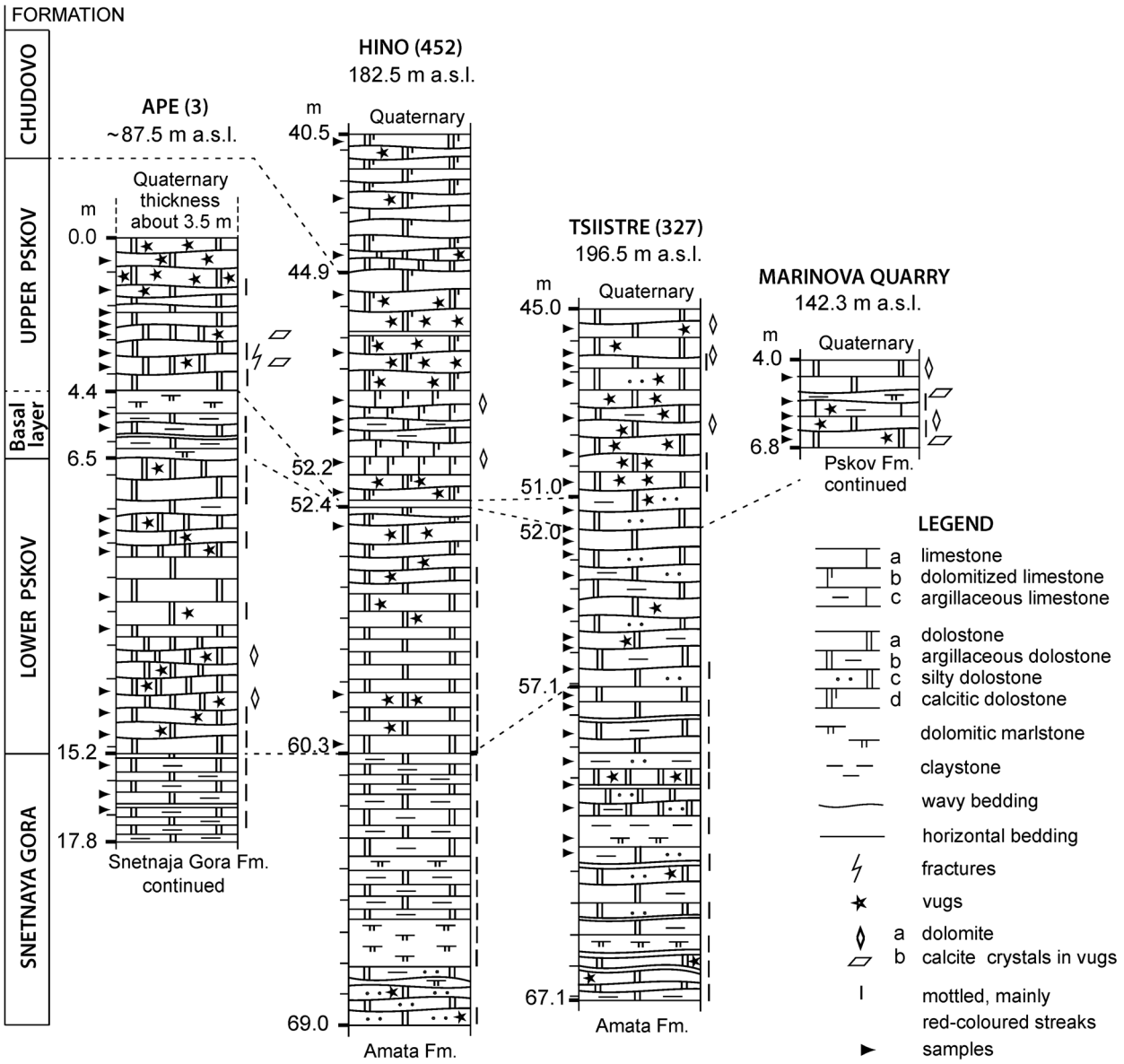

Fig. 2. Correlation of the Plavinas RS (Upper Devonian, Frasnian Stage) in the studied sections. Data from the Ape and Hino sections are first published. Detailed description of the Tsiistre drill core is available in Põldvere (2007). The walls of Marinova quarry described by Põldvere (2012). The drill core and quarry site elevation are in metres above sea level (m a.s.l.).

scanning electron microscope (SEM) Zeiss EVO MA 15 (Carl Zeiss Inc.) in the backscattered electron imaging (BSE) mode. Chemical composition was analysed with the energy dispersive X-ray spectrometer INCAx-act (Oxford Instruments Plc) attached to SEM, at 20 kV acceleration voltage and 1 nA beam current. Cathodoluminescence (CL) effects were studied in 16 thin sections, with the cold cathode CL stage CL8200 Mk5 (Cambridge Image Technology Ltd) attached to an optical microscope, at 20 kV acceleration voltage and 0.2 A beam current.

The bulk chemical composition of 63 rock samples was determined by XRF spectrometry on the Bruker S-4 spectrometer. Insoluble residue (IR) was measured by gravimetry; MgO and CaO contents were measured by titration.

The mol% content of $CaCO_3$, $MgCO_3$ and $FeCO_3$ in dolomite was calculated from the results of XRF and chemical analyses in 51 samples where X-ray diffractometry did not reveal the presence of other carbonate minerals. Twenty-one samples were subjected to X-ray diffractometry measurements for identification of carbonate minerals and d_{104} position of dolomite with the HZG-4 diffractometer.

Various carbonate phases determined by petrography were sampled for C and O isotope study. A total of 52 measurements of 38 samples were made. Carbon and oxygen isotope analyses were performed with the GasBench II preparation line connected to the Thermo Scientific Delta V Advantage mass spectrometer. The material was powdered and treated with 99% phosphoric acid at 70 °C for 2 h. The results are given in the usual δ-notation, as per mil deviation from the VPDB standard. Reproducibility of duplicate analyses was generally better than 0.1‰. All laboratory analyses were performed in the Institute of Geology at Tallinn University of Technology. All rock samples and thin sections, studied for this paper, are deposited at the same institute (repository acronym GIT).

RESULTS

Distribution of rock types, depositional environments and stratigraphy

On the basis of lithological and sedimentological characteristics, the section was divided into five units: Snetnaya Gora Fm, Lower Pskov, basal part of the Upper Pskov and Upper Pskov units, and Chudovo Fm (Fig. 2; Table 1). New analytical data obtained during the present study were used for detailed lithostratigraphical correlation of the examined sections. Compared to earlier publications (Kajak 1997), the boundaries of the Snetnaya Gora and Pskov Fms in the Tsiistre drill core and of the Pskov and Chudovo Fms in the Hino drill core were adjusted: the former was elevated by 2.1 m and the latter lowered by 4.4 m.

The 2.5–9 m thick Snetnaya Gora Fm is characterized by horizontal thin-bedded, usually platy dolostone (thickness of laminae 1–4 cm). The laminae have even or slightly uneven planes and different colour shades, with alternation of light grey, yellowish-, violetish- and greenish-grey interbeds (Fig. 3A). In places bedding planes are enriched in silty particles, and scattered quartz particles are present in matrix. The rock contains argillaceous and dolomitic clay interbeds (Fig. 2), including remarkable 1–3 mm thick interbeds of dolomitic siltstone with a modest concentration of iron oxides. The rock is mainly unfossiliferous, with the IR content of 12–25%. There occur, however, rare, up to 20 cm thick interbeds of massive dolostone with IR <2%. This succession records a transgressive–regressive cycle of sedimentation in the initial phase of transgression (Wendte & Uyeno 2005). The occurrence of detrital particles suggests the presence of a nearby clastic source.

The 6–9 m thick Lower Pskov unit is composed of intercalating variegated thin-bedded to light grey thick-bedded layers (Fig. 3B). Variegated levels are usually

Table 1. Character of lithological units

Unit	Thick-ness, m	Rock types	Thickness of beds, cm	Insoluble residue, %	$MgCO_3$, mol% dolostone (mean)	$FeCO_3$, mol% dolostone (mean)	MnO, % dolostone (mean)	$\delta^{13}C$, ‰ dolostone	$\delta^{18}O$, ‰ dolostone	Depositional facies
Chudovo	4.8	Intercalated Ca-rich vuggy dolostone and limestone	0.1–50	Dolostone 10–16 limestone 5	40.25	0.45	0.047	–	–	Nearshore marine
Upper Pskov	4.4–7	Dolostone, in places limestone interbeds	2–10	1.5–5.5	47.45	0.57	0.047	0.18	–5.09	Nearshore marine, regressive trend
Basal layer of Upper Pskov	0.2–1.9	Dolomitic marlstone	1–2	13–42	47.05	0.96	0.062	–	–	Shallow marine
Lower Pskov	5–10	Vuggy dolostone, in the uppermost part Ca-rich	0.5–40	2–13	48.0	0.65	0.058	–0.42	–4.55	Shallow marine, relative sea-level highstand
Snetnaya Gora	2.5–9	Thin-bedded dolostone	1–4	12–25	47.95	1.25	0.105	–2.47	–3.87	Shallow marine, transgressive

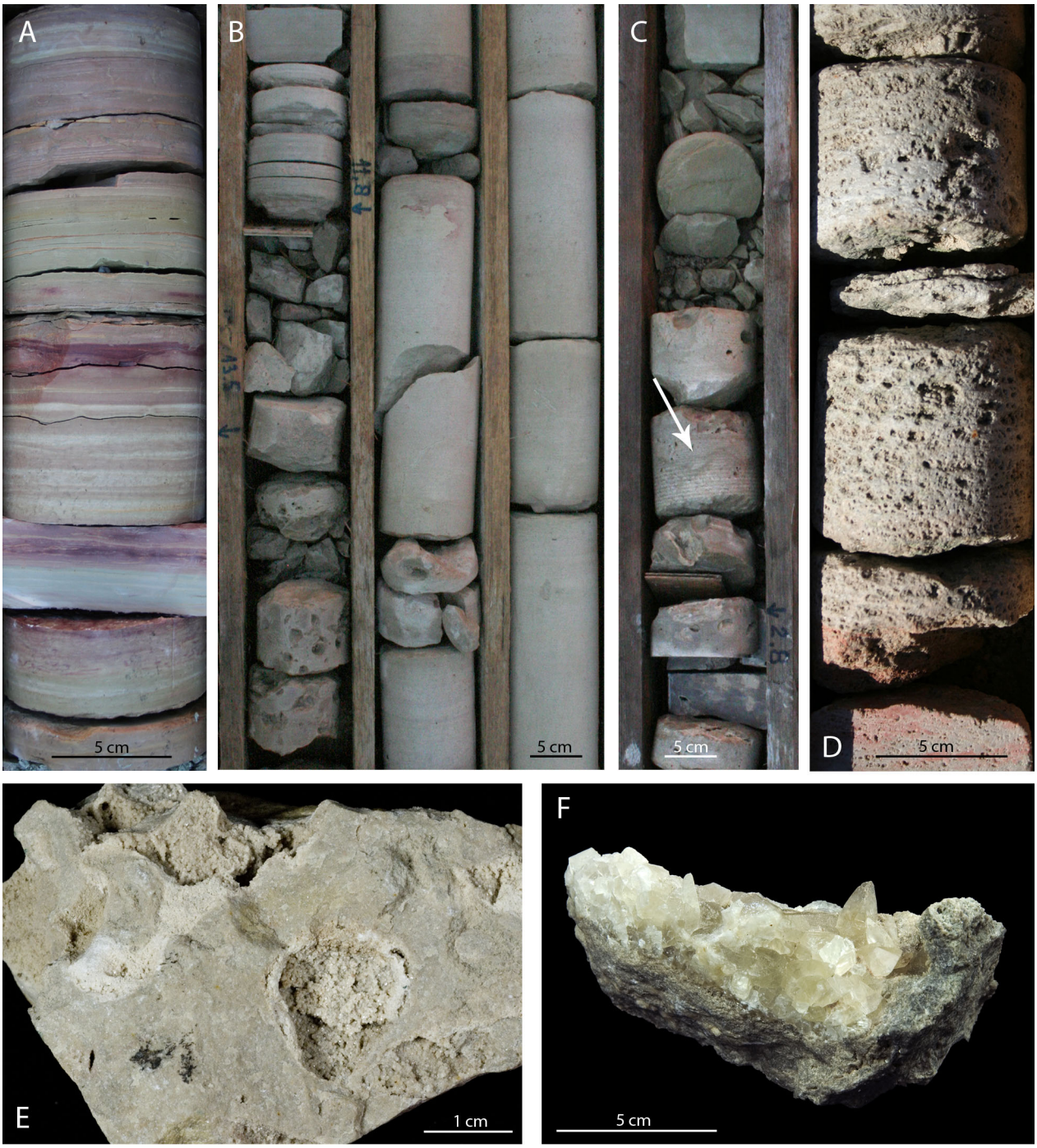

Fig. 3. Photographs illustrating the lithology of the studied rocks. (**A**) Platy dolostone of the Snetnaya Gora Fm, Ape drill core, 16.3–16.7 m. (**B**) Variegated porous and thin-bedded (left) and thick-bedded compact (right) dolostone, typical of the Lower Pskov unit, Ape drill core, 9.4–12.5 m. (**C**) Lenticular-vavy bedded very finely crystalline vuggy dolostone with stylolite planes (arrow) occurring in the Upper Pskov unit, Ape drill core, 2.0–2.8 m. (**D**) Sucrosic dolostone, characteristic of the Upper Pskov unit, Ape drill core, 1.2–1.5 m. (**E**) Moldic pores in the Upper Pskov unit; Tsiistre drill core, 46.0 m, GIT 156-305. (**F**) Calcite filling in the Upper Pskov unit, Marinova quarry, GIT 443-555.

cavernous. Vugs of irregular shape (usually 0.1–2 cm, in some cases up to 5 cm in diameter) make 3–10% of the rock (Figs 2, 3B). Light grey dolostone layers (mainly 20–40 cm thick; Fig. 3B) contain fine vugs. The dolostone in the topmost part of the unit is Ca-rich. The content of IR varies from 2% to 13% (Table 1). The unit was most probably deposited under stable conditions during relative highstands of sea level in shallow marine conditions. Porosity is obviously mainly related to dolomitization.

The basal layer of the Upper Pskov unit in the Ape section consists of a 2 m thick complex of grey dolomitic marlstone and clayey thin-bedded dolostone. In the Tsiistre section this level is represented by 1 m thick argillaceous dolostone (IR 13%) and in the Hino section by 0.2 m thick dolomitic marlstone.

The about 7 m thick Upper Pskov level follows higher in the section. It is represented by thin- (1–5 cm) to medium-bedded (5–19 cm) rocks. Often lenticular-wavy bedding and stylolitic planes are observed (Fig. 3C). Very finely to coarse-crystalline dolostones alternate, containing vuggy intervals which often have sucrosic texture (Fig. 3D). Dolostone layers contain moldic vugs (Fig. 3E). Some vugs are occluded with calcite or dolomite fillings (Fig. 3F). Obviously, here the porosity is largely caused by karst phenomena. Dolostone layers intercalate with limestone interbeds, especially in the Hino drill core and Marinova quarry sections. Skeletal debris of marine fauna is often recorded in limestone beds (Fig. 4A). However, part of the limestone beds are unfossiliferous, with widely varying crystal size and locally preserved rhombic dolomite crystals in Marinova quarry (Fig. 4B). These limestone beds are probably dedolomization product, usually accompanied by brecciation. The Upper Pskov level has a low content of IR (1.5–5%; Table 1). The Upper Pskov unit with interlayers of sucrosic dolostones is characteristic of shelf carbonates and is also present (Choquette et al. 1992; Maliva et al. 2011) in other shallow marine platform environments.

The Chudovo Fm occurs only in the topmost part of the Hino section and is represented by intercalation of Ca-rich dolostones and limestones (Fig. 2). Limestone is very finely crystalline (0.01–0.02 mm), with cloudy matrix under a microscope, fine-nodular (0.1–0.2 mm, rarely up to 1 mm) and rich in fossil remains up to 3 mm in size. Besides, limestone contains rounded areas (0.2–1 mm) filled with transparent irregularly shaped calcite crystals (0.08–0.2 mm) and is penetrated by wavy, often branching fractures (cross section 0.04–0.8 mm) filled with irregularly shaped medium- to coarsely crystalline (0.2–0.4 mm) calcite crystals showing the same CL colour and intensity as their host limestone. Some crystals are slightly zoned. The content of insoluble residue is 1–15% in dolostones and <5% in limestones (see Table 1).

Dolomite petrography and distribution

The lower units (Snetnaya Gora and Lower Pskov) of the examined sections are completely dolomitized, while the upper units contain Ca-rich dolostone and limestone interlayers (Table 1, Figs 2, 5A). Petrographic information on different types of dolomite was obtained by using light, CL and SEM microscopy. Dolomite textures were classified after Sibley & Gregg (1987). Six types of dolomites (described below) were distinguished, based on crystal size and texture, crystal boundary shape, CL properties and association with dolostone matrix (Fig. 6). The dolomites are commonly stoichiometric, with low iron and manganese contents (Fig. 5A–C).

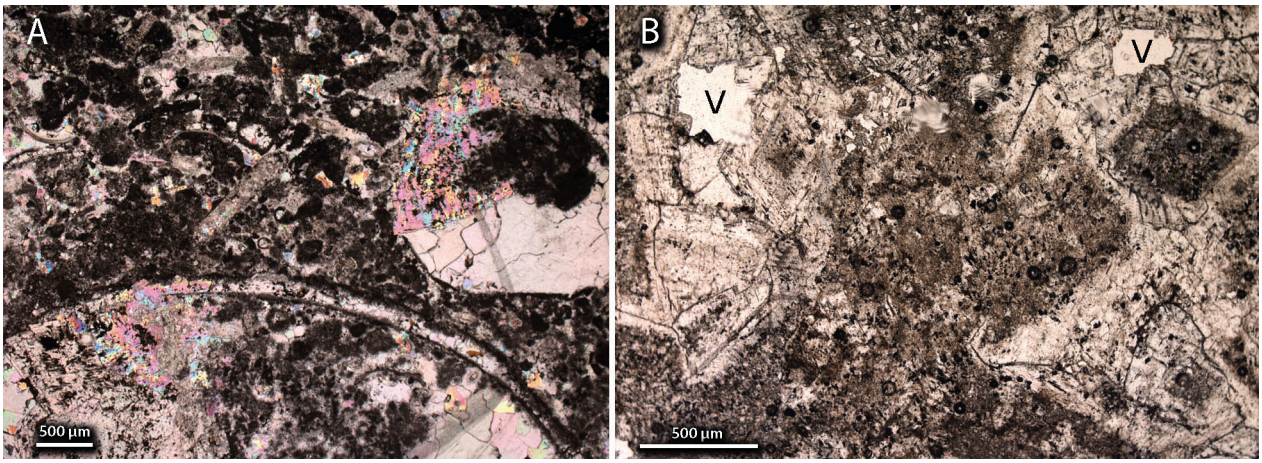

Fig. 4. Thin section photomicrographs of (**A**) Plavinas limestone and (**B**) limestone precipitated during dedolomitization. The limestone is rich in fossil remains, while in matrix of unfossiliferous vuggy (V in part B) dedolomite some remnant dolomite zoned rhombs are preserved. A, Hino drill core, 49.4 m, GIT 441-640; B, Marinova quarry 4, GIT 443-562.

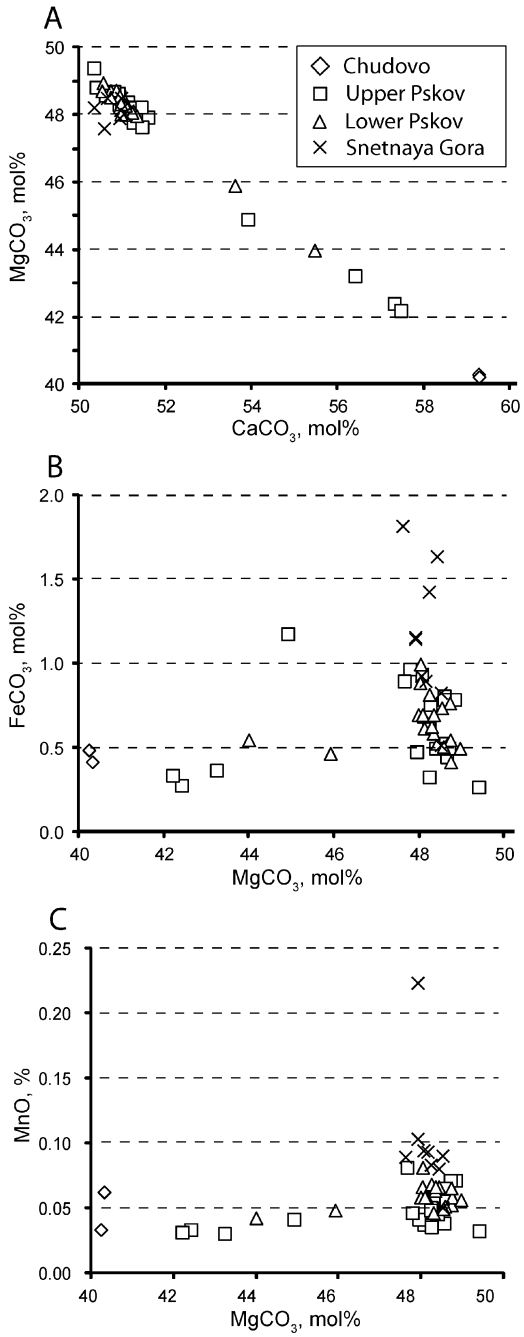

Fig. 5. Chemical composition in (**A**) mol% $CaCO_3$ to mol% $MgCO_3$, (**B**) mol% $MgCO_3$ to mol% $FeCO_3$, and (**C**) mol% $MgCO_3$ to %MnO.

Type 1. Very finely to finely crystalline dolomite in laminated silty dolostone

Crystals (30–60 μm in diameter) in slightly cloudy rock are subhedral and usually unzoned. Irregularly patchy (0.5–2 mm) matrix is slightly pigmented by Fe-hydroxide. Pigmentation is commonly concentrated along bedding planes (Figs 3A, 6A). Cloudy, very finely crystalline (10–15 μm) dolomite interlayers (1.6–4 mm) alternate with semitransparent finely crystalline (20–60 μm) dolomite laminae (0.8–1.2 mm). Semitransparent layers contain rare medium-crystalline zoned euhedral dolomite crystals. Silty quartz grains (50–70 μm) form about 1% or less of the rock. Quartz grains are clear, usually rounded. Rare fine irregular-shaped vugs (0.1–0.2 mm) are found. Type 1 dolomite is present only in the Snetnaya Gora Fm where it is a dominant feature (Table 2).

Type 2. Very finely crystalline dolomite

Very finely (5–10 μm) crystalline dolomite occurs in a lenticular-wavy bedded interval in the lower part of the Upper Pskov unit of the Ape section. The rock with homogeneous distribution of crystals and dull CL is unfossiliferous, penetrated by abundant irregular-shaped fine vugs (0.2–0.6 mm, in some cases up to 2 mm), often oriented along bedding planes. Vugs are rimmed or filled with calcite crystals, occasionally surrounded by Fe-hydroxide pigmentation (Figs 6B, 7A). Scattered pigmented patches are found in rock matrix. Cathodoluminescence studies indicate that part of the vug-filling calcite crystals at the pore walls are enriched in Mn (Fig. 7B). Energy dispersive spectrometry (EDS) revealed siderite crystals among calcite in vug fillings (Fig. 7C).

Type 3. Concentric zoned dolomite crystals floating in finely crystalline limestone

Medium- (60–100 μm) to coarsely (60–1200 μm) crystalline euhedral to subhedral dolomite crystals are embedded in very finely crystalline (about 10 μm) limestone matrix rich in fossil remains. The outlines of dolomite crystals are mainly planar, but some dolomite crystals have slightly serrated outlines (Figs 6C, 8, 9). Most of the dolomite crystals have a cloudy core (200–600 μm) surrounded by a clear white rim (20 μm) with planar sides well seen under a light microscope. In some crystals 2–4 additional white zones (<10 μm) are visible in the core. In the CL image the white rim is hardly seen (Fig. 8A, B). The white rim is coated by a cloudy dark rim (100–150 μm), mainly with unclear outer surfaces. This dark rim often contains 2–3 tiny, sometimes hardly recognizable light zones. The outer part of the crystal is represented by a clear transparent rim (20–40 μm; Figs 6C, 8A), sometimes with a tiny fragmentary dark zone in the outer part visible in CL (Fig. 8B). In total up to 20 zones were counted in a single crystal. Irregular-shaped voids often occur inside zoned crystals, mostly in the core, but also within the outer zones (Fig. 8C). In some places wavy extinction of dolomite crystals is recorded. Type 3 dolomite is

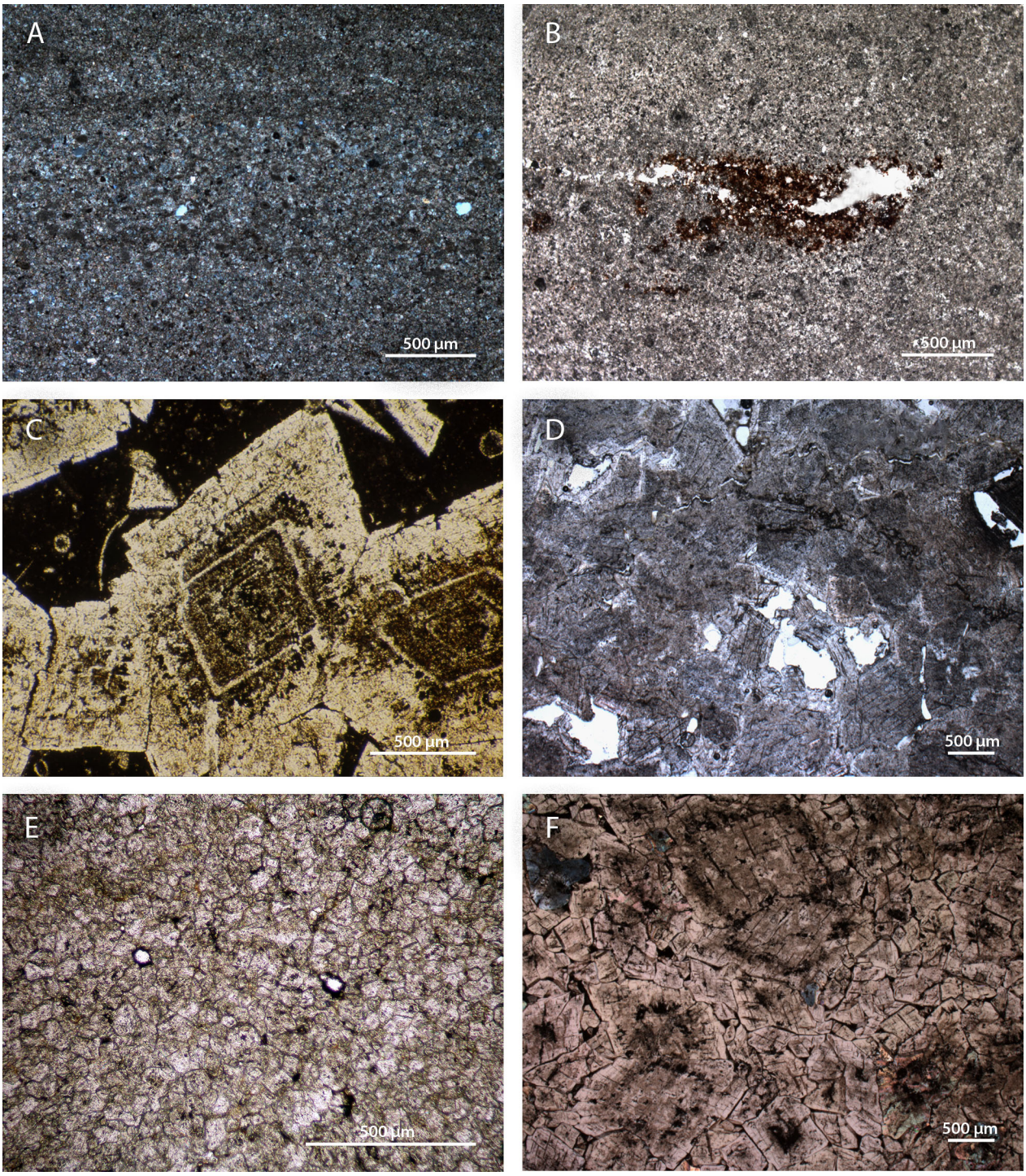

Fig. 6. Thin section photomicrographs in cross-polarized light illustrating different types of dolomite crystals present in the studied rocks. (**A**) Type 1 dolomite, Snetnaya Gora Fm, Ape drill core, 16.6 m, GIT 442-602. (**B**) Type 2 dolomite, Upper Pskov unit, Ape drill core, 3.8 m, GIT 442-500. (**C**) Type 3 dolomite, Upper Pskov unit, Hino drill core, 45.8 m, GIT 441-637. (**D**) Type 4 dolomite, Upper Pskov unit, Ape drill core, 1.4 m, GIT 442-585. (**E**) Type 5 dolomite, Lower Pskov unit, Tsiistre drill core, 52.9 m, GIT 550-4. (**F**) Type 6 dolomite, Lower Pskov unit, Hino drill core, 53.0 m, GIT 441-644.

Table 2. Characteristics of dolomite types

Dolomite type	Crystal size, μm	Crystal habitus	Zonation	Distribution	Suggested environment
Type 1 Finely crystalline, with silty interbeds	30–60	Subhedral	Unzoned	Snetnaya Gora	Marine-meteoric in the periphery of the sedimentary basin
Type 2 Very finely crystalline	5–10	Subhedral	Unzoned	Upper Pskov (Ape)	Shallow-marine subtidal and supratidal
Type 3 Isolated rhombs floating in limestone matrix	60–1200	Euhedral to subhedral, planar; in places with serrated outlines	Concentric zoned	Upper Pskov (Hino)	Marine-meteoric
Type 4 Sucrosic	400–800	Euhedral to subhedral, planar	Zoned	Upper Pskov	Shallow-burial dolomitization
Type 5 Fine- to medium-crystalline	50–150	Subhedral to euhedral, planar	Zoned	Lower Pskov, in places Snetnaya Gora	Subtidal to supratidal
Type 6 Inequigranular	200–1200	Subhedral to euhedral, planar; in places anhedral, with serrated or rounded outlines	Zoned	Lower and Upper Pskov, in some places Chudovo	Shallow-burial dolomitization

non-stochiometric (Ca dominating over Mg) and is found in the Upper Pskov unit of the Hino section (Table 2). Similar to the Upper Devonian of Estonia, this type is also present in incompletely dolomitized levels in other regions and stratigraphical levels (Dix 1993; Kallaste & Kiipli 1995).

To quantify the chemical characteristics of the concentric zoned dolomite crystals, two crystals (samples Hino 45.8 and 49.0 m) were subjected to electron microprobe analysis using EDS linescan across a rhomboedra, which gave a profile of relative concentrations of elements in dolomite (Fig. 9). In addition, EDS point analyses were made on different zones of the crystal in order to reveal the fully quantitative composition of dolomite. Five zones of crystal growth can be distinguished in the geochemical profiles presented in Fig. 9. The calcium-rich nucleation site (zone 1) is surrounded by microcrystalline calcite and dolomite grains (zone 2) with highly variable contents of Ca and Mg (Fig. 9) and random occurrence of Si and K. The central part of the crystal is surrounded by a growth band (zone 3) with straight faces, which are commonly parallel to external crystal faces. This band, ranging from a couple of to several micrometres in thickness, consists of pure dolomite without impurities and is recognizable under a light microscope as a white zone (Figs 6C, 8A). Zone 4 resembles zone 2, containing scattered patches of calcite and dolomite material. In comparison with zone 2, the content of Mg is somewhat higher and supplement of the detrital component (Si, K) is lower. The outer surface of zone 4 is unclear. The cortex of the dolomite crystal (zone 5) is represented by a clear pure dolomite band with rare fine calcite patches. The content of Fe, Mn, Sr, Cl and Na is almost uniformly low within the dolomite crystal and does not show any clear trend. Energy dispersive spectrometry point analyses (Fig. 9) show that dolomite particles in zone 2 are highly calcitic, while these of zones 3 and 5 have quite similar Ca/Mg ratios representing moderately calcitic dolomite.

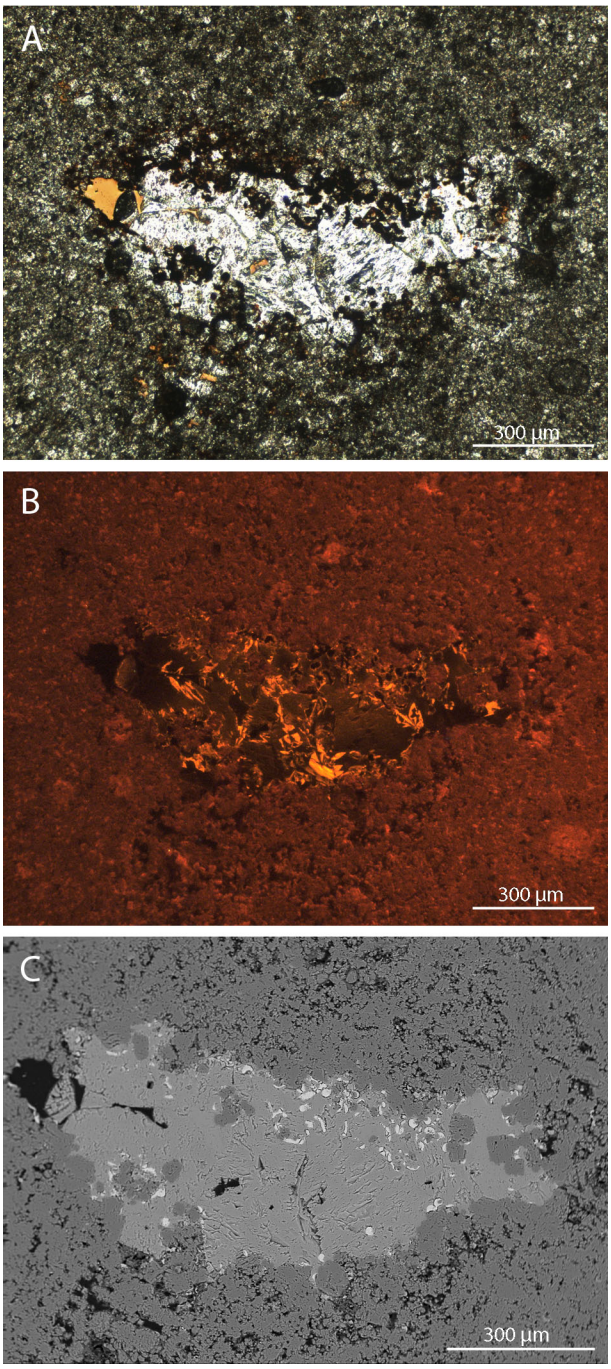

Fig. 7. Calcite-filled vug in very finely crystalline dolostone in light microscope (**A**), cathodoluminescence (CL) (**B**) and scanning electron microscopy (SEM) (**C**). In CL some calcite crystals show Mn content (clear orange CL colour in the colour image; white crystals in the black-and-white image). Energy dispersive spectrometry revealed tiny siderite crystals in the rimming parts of the calcite filling (white particles in grey matrix in SEM). Ape drill core, 3.8 m, GIT 442-590.

Type 4. Sucrosic dolomite

This type is represented by coarsely crystalline (400–800 µm) dolomite with planar euhedral to subhedral zoned crystals. The non-luminescent cloudy crystal core is surrounded by a dull luminescent clear rim (10–100 µm). Dolomite crystals have often internal discontinuities and corroded core surfaces (Figs 6D, 10A). According to EDS, the Ca^{2+}/Mg^{2+} ratio of the cloudy core and clear rim are similar. The cloudy core contains Si, pointing to the occurrence of inclusions. Deformed, wavy extinction of dolomite crystals is frequent. The rock is strongly vuggy (Fig. 3D). Intercrystalline porosity (20–25%) is high (Fig. 6D), including vugs with irregular outlines (0.4–2 mm, in some cases up to 4 mm; Figs 3D, 6D, 10). The pore surfaces are rimmed with tiny dolomite crystals exhibiting bright red CL colour (Fig. 10B, C). In places wavy sutured planes penetrate the rock (Fig. 10A). In CL, the sutured planes have bright red colour like the crystals rimming pore surfaces (Fig. 10B). Illite has precipitated in intercrystalline spaces (Fig. 10D). Type 4 dolomite has been recorded in the topmost part of the Upper Pskov unit of the Ape, Tsiistre and Marinova sections.

Type 5. Finely to medium-crystalline dolomite

Fine to medium-sized euhedral to subhedral planar crystals (50–150 µm) are usually zoned. Non-luminescent cloudy crystal cores of variable size and shape have clear outer boundaries surrounded by clear moderately luminescent rims (20–50 µm). The core shape varies from a perfect rhombohedra to nearly round core and often matches the outline of the crystal (Figs 6E, 11A, B). The rock is often penetrated by fractures and fine irregularly angular and rounded vugs (0.1–0.2 mm, in some cases up to 0.6 mm; Figs 6E, 11A). In places vugs are surrounded by a yellowish-cloudy rim (Fig. 6E). Type 5 dolomite occurs in the Lower Pskov unit, but also as interlayers in the Snetnaya Gora Fm (Table 2).

Type 6. Inequigranular dolomite

Inequigranular dolomite contains zoned dolomite grains, typically 200–1200 µm in size. The grains are planar, subhedral and euhedral, often also anhedral with serrated or rounded outlines (Figs 6F, 12A). Dolomite crystals have a semitransparent or cloudy core surrounded by an indistinctly terminated Fe-rich level (0.04–0.08 mm), rimmed by a clear outer cortex (10–20 µm). The core may be zoned as well (Fig. 12A, B). A total of five zones have been counted. In places rare irregular-shaped angular vugs (0.2–1 mm) are found. Many crystals are deformed owing to wavy extinction. Cathodoluminescence analysis reveals a dark red band in the centre of the mainly dull

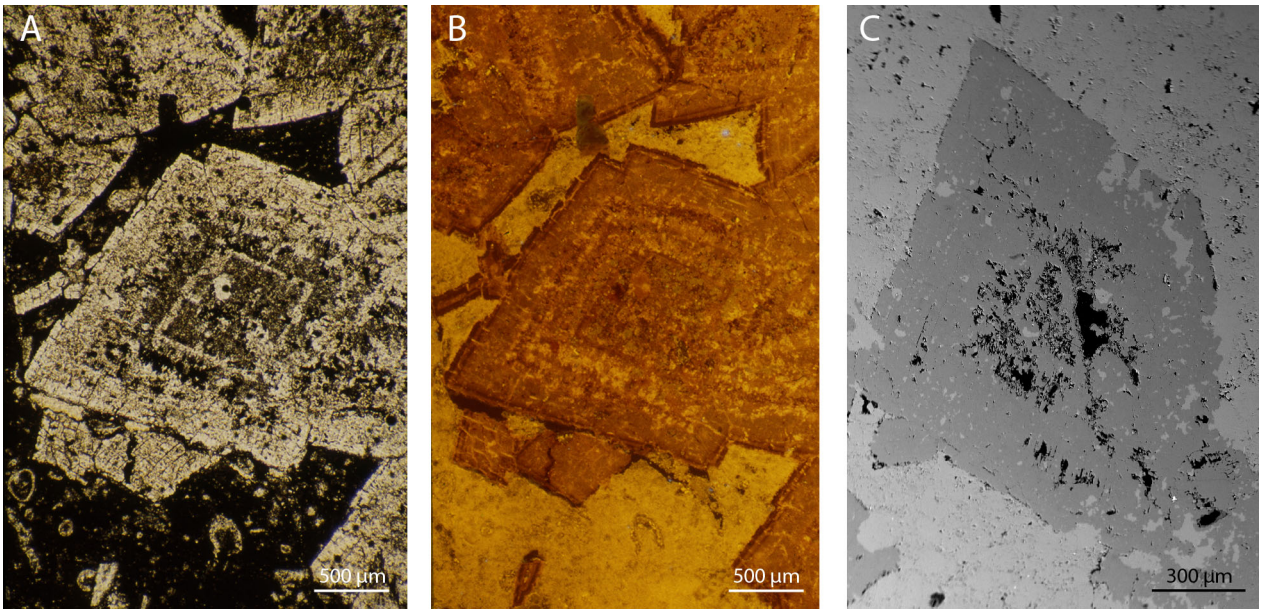

Fig. 8. Concentric zoned dolomite rhomb (type 3) floating in fossil-rich limestone matrix in light microscope (**A**), cathodoluminescence (CL) (**B**) and scanning electron microscopy (SEM) in the backscattered electron imaging mode (**C**). In CL crystals are surrounded by dark outer cortex. The SEM micrograph shows abundant tiny vugs (black) in the centre the crystal. Some of the vugs are oriented along zoned planes inside the crystal. (A) and (B) Hino drill core, 45.8 m, GIT 441-637; (C) Hino drill core, 49.0 m, GIT 441-639.

red crystal. The vugs are surrounded by a dark red rim (Fig. 12B). Some rusty pigmentation is observed between the grains. Dolomite in the matrix rock is non-stoichiometric.

Void-filling dolomite and calcite

The studied carbonate rocks contain numerous vugs and fractures (Fig. 3). Voids in the Lower Pskov section are mainly open. In the upper part of the sequence (Upper Pskov, Chudovo) vugs and fractures are partly or completely filled with dolomite, some of them with calcite (Figs 2, 3, 7). Vug-filling dolomite is composed of coarse transparent euhedral crystals with planar faces (up to 1.5 mm in size; Fig. 13). According to EDS analysis, the Ca/Mg ratio of void-filling dolomite crystals shows no difference from that of matrix dolomite crystals.

The crystal size of void-filling calcite varies widely. In some cases large voids are filled with clear coarse-grained (up to 5 mm) calcite crystals with perfect crystal faces (Fig. 3F). Fine vugs are rimmed or occluded with clear subhedral and anhedral, often elongated, medium-crystalline (100–150 µm) calcite (Fig. 7).

Composition of mineral dolomite

Dolostones of the studied sequence contain mostly dolomite of nearly ideal stoichiometric composition (50.0–52.5 mol% $CaCO_3$; Fig. 5). Dolomite in rocks containing calcite or occurring not far from limestone interbeds is often Ca-rich, with 54–59 mol% $CaCO_3$. This regularity is evident from XRF and chemical data and confirmed also by XRD data. The d_{104} measurements revealed two clusters at 2.877–2.889 Å (close to the stoichiometric composition) and 2.901–2.903 Å (Ca-rich non-stoichiometric composition). Dolostones of the shallow-marine transgressive phase of the Snetnaya Gora Fm exhibit the highest $FeCO_3$ and MnO (probably partly bonded to the silicate component of the rock) concentrations among all formations (Fig. 5B, C). Dolomite in stratigraphically lower levels is closer to the stoichiometric composition (Fig. 5A), while interbeds of Ca-rich non-stoichiometric dolomites occur mainly in the upper part of the section (Upper Pskov and Chudovo Fms). Dolostones of the Chudovo Fm are extremely enriched in $CaCO_3$ (up to 59 mol%; Fig. 5A). The presence of calcian dolomites indicates the formation of dolomite from solutions with a relatively low Mg/Ca ratio and they are considered to have a near-surface origin (Török 2000). Planar rhombs of type 3 dolomite scattered in limestone matrix (Fig. 6C) are non-stoichiometric ($CaCO_3$ mol% >56). Inequigranular dolomite of type 6 is also non-stoichiometric and Ca-rich. However, dolomite is considered to become closer to stoichiometric composition during progressive recrystallization and characteristics of type 6 dolomite point to recrystallization processes.

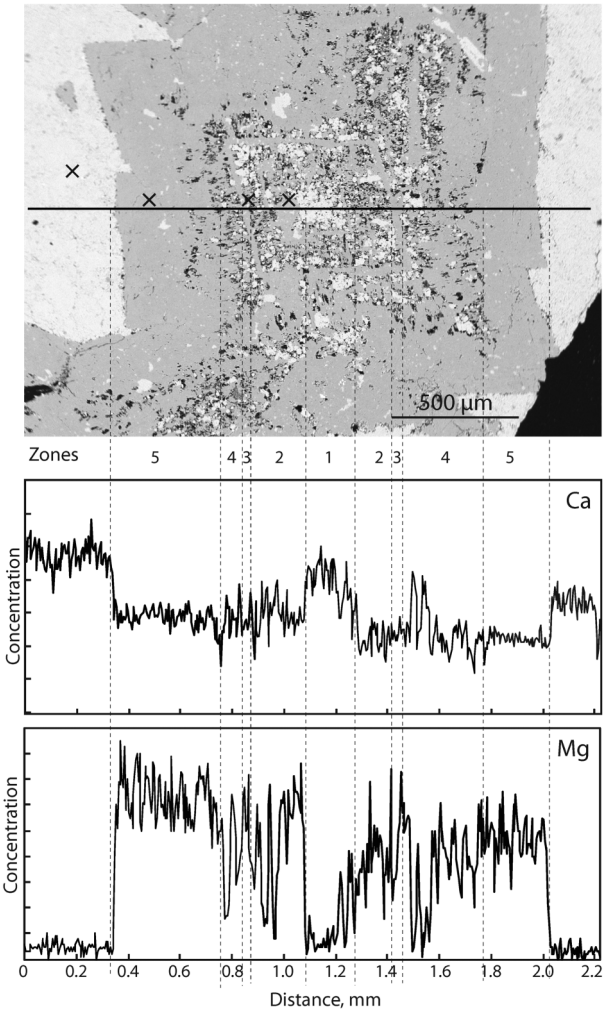

Fig. 9. Extremely variable concentrations of Ca and Mg along the transect line across the concentric zoned dolomite rhomb of type 3 analysed with the electron microprobe. The determined zones correspond to the zonation discussed in the text. The places of point analyses are marked with crosses. Hino drill core, 45.8 m, GIT 441-637.

In this case it is possible that the enrichment with Ca is connected with circulation of karst-related fluids during the late stage of diagenesis.

Stable oxygen and carbon isotopes

Stable oxygen and carbon isotope ($\delta^{18}O$, $\delta^{13}C$) results are summarized in Tables 3 and 4, crossplots are presented in Fig. 14. The $\delta^{13}C$ values of the dolostones/dolomites range from –4.48‰ to +0.99‰ and $\delta^{18}O$ values from –7.54‰ to –3.42‰. In limestones $\delta^{13}C$ ranges from –2.05‰ to –1.6‰ and $\delta^{18}O$ from –11.65‰ to –4.86‰. All these values are lower than typical of dolomites and calcites deposited directly from Frasnian seawater (Amthor et al. 1993), suggesting that Plavinas carbonate rocks were strongly modified by diagenesis (Fig. 14A).

The Upper Devonian sequence exhibits a positive excursion of $\delta^{13}C$ values and a negative trend of $\delta^{18}O$ values from the Snetnaya Gora Fm upwards (Fig. 14A, Table 3). These excursions represent one of the most prominent lowermost Frasnian excursions – the *Falsiovalis* Event (Buggisch & Joachimski 2006; van Geldern et al. 2006). On the other hand, the positive excursion of $\delta^{13}C$ values from the Snetnaya Gora Fm upwards may also be influenced by a transgression event (Buggisch & Mann 2004). Finely crystalline dolomite of the transgressive phase (type 1) is depleted in ^{13}C (–4.48‰ to –1.94‰), suggesting dolomite formed from mixed meteoric/marine fluid (Cioppa et al. 2003). Values of $\delta^{18}O$ vary slightly (from –4.35‰ to –3.98‰), pointing to stable temperature conditions during the formation of dolomite (Lumsden & Caudle 2001). Four of the six samples analysed from type 2 dolomites show similar values of $\delta^{13}C$ and $\delta^{18}O$, fluctuating in a narrow range. Two samples (Ape 2.8 and 13.2 m) are different, being depleted in ^{13}C and ^{18}O (Fig. 14B, Table 3). These samples differ from the others also by the abundance of open pores rimmed with authigenic dolomite crystals and most probably were overprinted by later diagenetic events.

The $\delta^{18}O$ values of rock with isolated dolomite rhombs floating in limestone matrix (type 3) are somewhat more negative in comparison with dolomite types 1 and 2, however, the value of $\delta^{13}C$ is similar to types 2 and 3 (Fig. 14B, Table 3). The depletion of ^{18}O values is connected with Ca-rich composition of the rock (Lavoie et al. 2005).

For sucrosic dolomites (type 4) 13 measurements of stable isotopes were made (Table 3). Most samples show $\delta^{13}C$ values from +0.99‰ to +0.46‰ and $\delta^{18}O$ values from –5.52‰ to –4.17‰. All samples that are depleted in ^{13}C (up to –1.63‰) contain dolomite- or calcite-filled voids. Some samples with calcite-filled voids show extremely varying $\delta^{18}O$ values (from 7.52‰ to –3.42‰; Fig. 14B, C, Table 3).

The $\delta^{13}C$ and $\delta^{18}O$ values of types 4 and 5 dolomites partly overlap. The values of $\delta^{18}O$ range from –4.92‰ to –4.01‰, but unlike type 4, most of the $\delta^{13}C$ values of type 5 are negative, pointing to the formation of mixing meteoric/marine water conditions.

Low $\delta^{13}C$ values, accompanied by variable $\delta^{18}O$ signatures in two analysed limestone interbeds (Marinova 3 and 4), indicate dedolomitization origin of these rocks. The $\delta^{13}C$ and $\delta^{18}O$ signatures of limestone are more negative (–1.65‰ to –2.05‰, and –4.86‰ to –11.65‰, respectively; Fig. 14B, Table 3). Relatively wide spacing of $\delta^{18}O$ values may be related to late recrystallization.

Stable isotope values of void-filling dolomite differ slightly from signatures of the host dolostones. The values

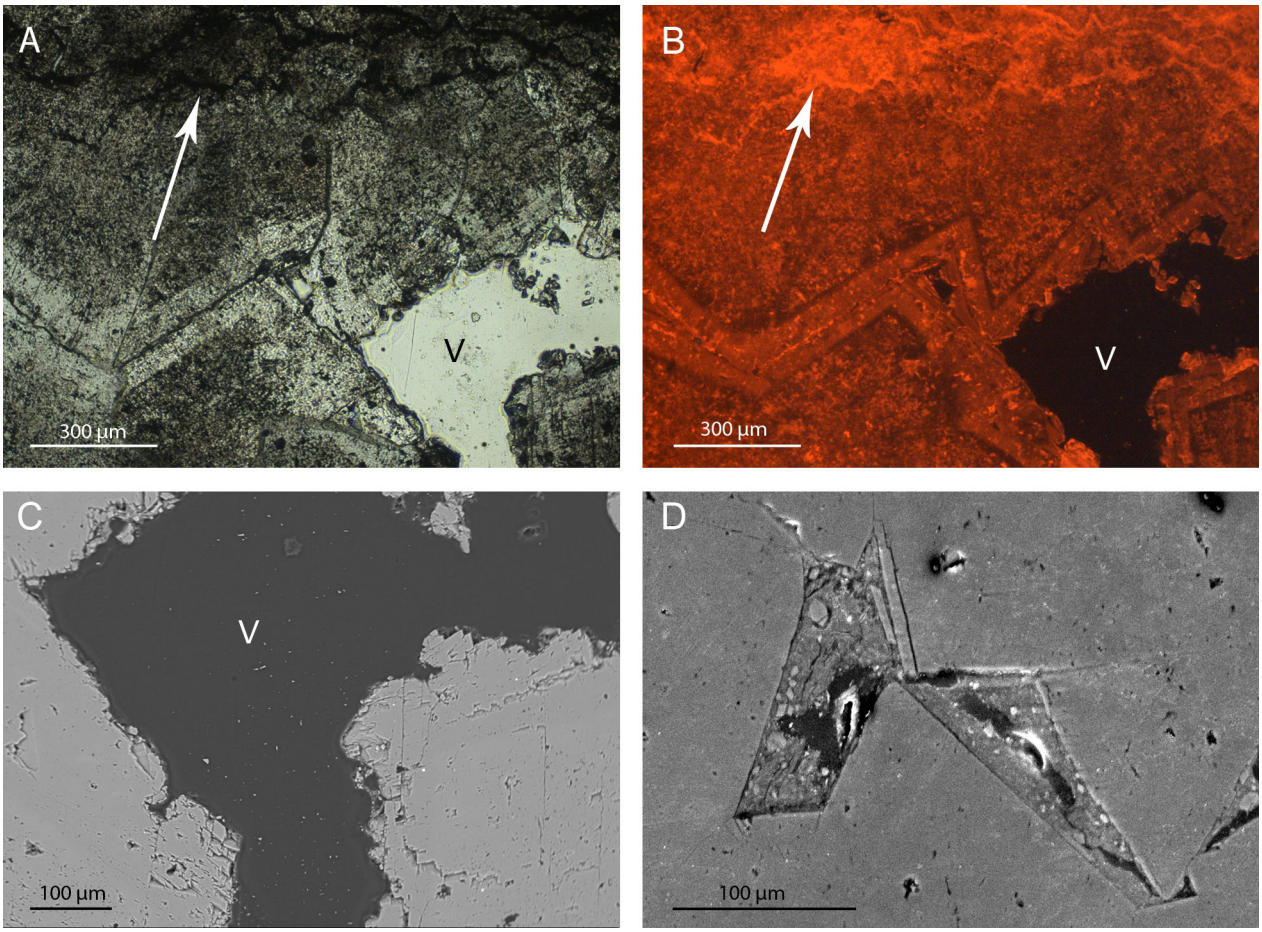

Fig. 10. Sucrosic dolomite in light microscope (**A**), cathodoluminescence (CL) (**B**) and scanning electron microscopy (SEM) in the backscattered electron imaging (BSE) mode (**C**). In light microscope and CL views a low-amplitude stylolite is observable (arrow). The vug (V) is lined with tiny crystals exhibiting in CL brightly luminescent colour similar to the stylolite plane, Ape drill core, 1.4 m, GIT 442-585. (**D**) Illite filling in the intercrystalline pore space of sucrosic dolomite, SEM in the BSE mode, Tsiistre drill core, 47.2 m. GIT 441-419.

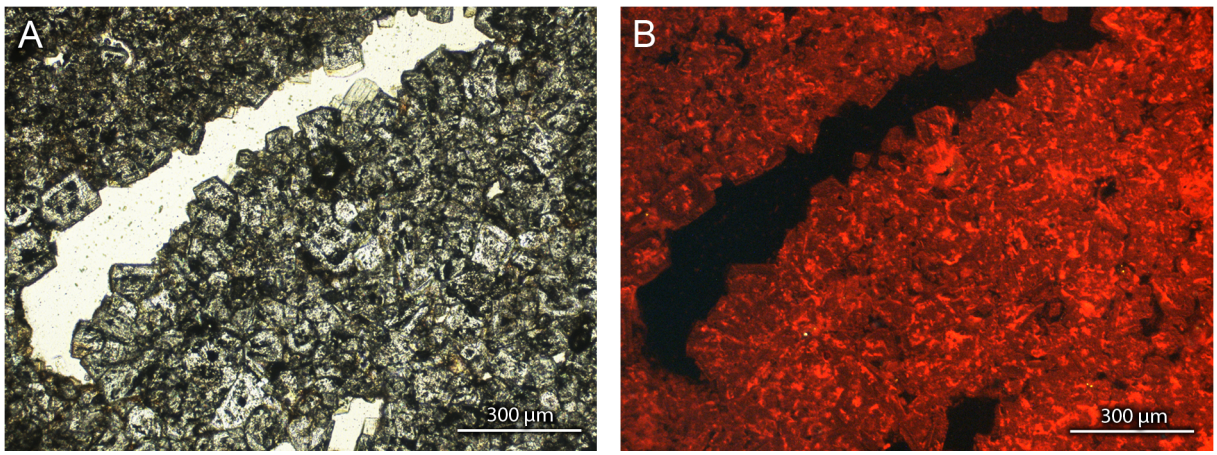

Fig. 11. Paired thin section photomicrographs of type 5 dolomite in light microscope (**A**) and cathodoluminescence (**B**). The rock-penetrating fracture is without any rimming features. Tsiistre drill core, 55.5 m, GIT 550-5.

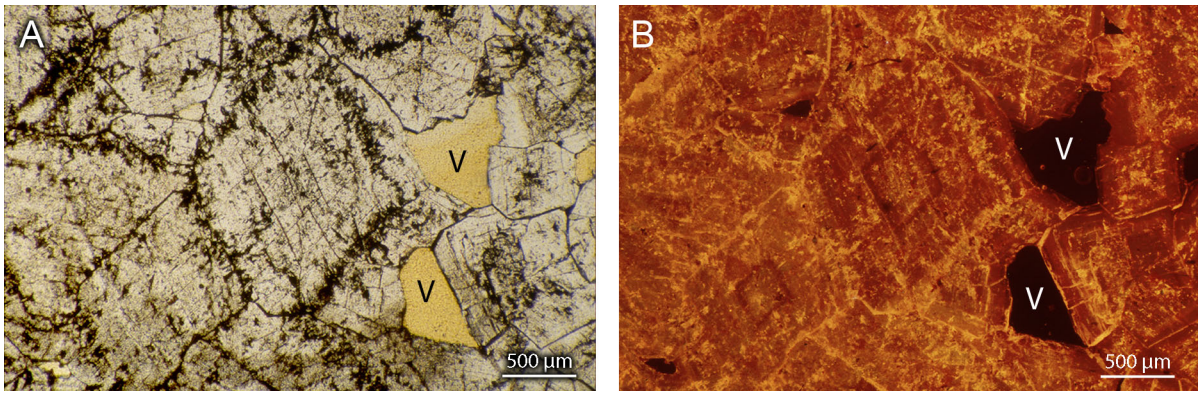

Fig. 12. Paired thin section photomicrographs of type 6 dolomite with vugs (V) in crossed polars (**A**) and cathodoluminescence (**B**). Hino drill core, 52.0 m, GIT 441-643.

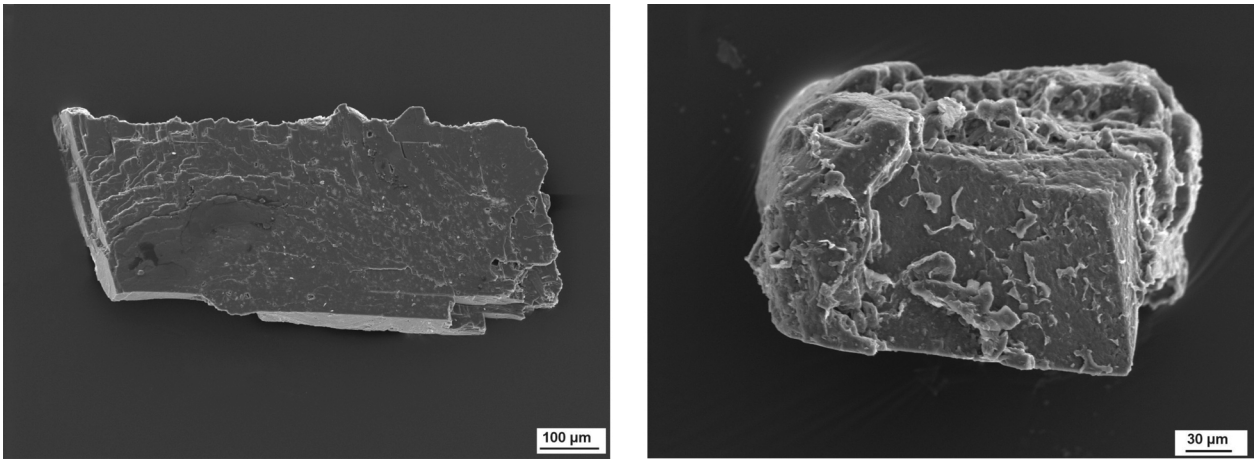

Fig. 13. Void-filling dolomite crystals in the Upper Pskov unit in scanning electron microscopy (backscattered electron imaging mode). Tsiistre drill core, 47.2 m, GIT 441-419.

of $\delta^{13}C$ and $\delta^{18}O$ range from −1.0‰ to +0.91‰ and from −5.55‰ to −4.62‰, respectively, partly coinciding with dolomite types 2–5 (Fig. 14B, C). Coeval large differences in isotopic composition exist between void-filling calcite and host rock, indicating the formation of calcite at later stages of diagenesis. Calcite fillings generally yield the lowest $\delta^{18}O$ and $\delta^{13}C$ values (Fig. 14C, Table 4). Low $\delta^{18}O$ values of authigenic components have been attributed to precipitation from fluids containing significant amounts of isotopically light fresh water, which is typical of karst-related fluids (Török 2000; Nader et al. 2008).

DISCUSSION

The investigated Plavinas carbonate deposits were affected by multistage long-lasting dolomitization events. The measured stable isotope values differ essentially from those predicted for dolomites and calcites that deposited directly from Frasnian seawater, suggesting that rocks were modified by diagenesis (Fig. 14). Multistage dolomitization history is supported by the presence of limestone interlayers in sequences of the Upper Pskov unit and Chudovo Fm. If dolostones were formed during a single episode of pervasive alteration, the entire section would consist of dolostone. Vug- and fracture-filling dolomite precipitated from solutions that migrated through the Plavinas rock. Multiple episodes of dolomitization created different generations of dolomite crystals (Fig. 6). Passing through various diagenetic phases, early diagenetic features are obliterated (Warren 2000). Therefore, the dating of dolomitization events and the paragenetic sequence of diagenetic processes is complicated and we are able to propose only some preliminary interpretations of the

Table 3. Carbon and oxygen isotope data of the studied rocks

Unit	Section	Depth, m	Rock type	$\delta^{18}O$, ‰	$\delta^{13}C$, ‰
Upper Pskov	Tsiistre	45.6	4	–5.14	0.97
	Tsiistre	46.8	4	–4.99	0.93
	Tsiistre	47.2	4	–4.78	0.94
	Tsiistre	48.3	4	–4.77	0.99
	Tsiistre	49.6	4	–4.93	–0.9
		49.6a	4	–4.52	–0.48
	Tsiistre	50.5	4	–4.17	–0.25
	Ape	0.7	4	–5.02	0.52
	Ape	1.4	4	–5.38	0.48
	Ape	2.2	2	–4.23	0.48
	Ape	2.5	2	–4.17	0.51
	Ape	2.8	2	–5.31	0.06
	Ape	3.4	2	–4.27	0.42
	Ape	3.8	2	–4.54	0.69
	Marinova 5		4	–5.52	0.46
	Marinova 4		Limestone	–4.86	–1.65
	Marinova 3		Limestone	–11.65	–2.05
	Marinova 2		4	–6.38	–0.52
	Marinova 1A		4	–7.54	–1.01
	Marinova 1		4	–3.42	–1.63
	Hino	47.5	3	–5.7	0.5
	Hino	49.0	3	–5.48	0.18
		49.0a	3	–5.74	0.22
	Hino	51.0	3	–5.93	0.15
		51.0a	3	–5.28	0.54
Lower Pskov	Tsiistre	52.9	5	–4.83	–0.38
	Tsiistre	55.5	5	–4.78	–0.03
	Ape	8.2	5	–4.82	–0.68
	Ape	8.9	5	–4.01	–0.57
	Ape	9.2	5	–4.55	–0.39
	Ape	10.6	5	–4.35	–0.17
	Ape	11.7	5	–4.43	–0.12
	Ape	13.2	2	–5.15	–0.19
	Ape	14.0	5	–4.17	–0.43
	Ape	14.8	5	–4.42	–1.2
Snetnaya Gora	Ape	15.6	1	–4.06	–2.03
		15.6a	1	–3.98	–1.94
	Ape	16.6	1	–3.48	–2.44
	Tsiistre	57.6	1	–4.35	–4.48
	Tsiistre	59.4	1	–3.48	–1.45

diagenetic setting of the distinguished dolomite types and authigenic precipitations (Fig. 15).

Altogether, six types of dolomite, dedolomite precipitation, and void-filling dolomite and calcite were recognized. Type 1 dolomite occurs in thin laminated rock containing silty interbeds with an increased Fe content (Figs 3A, 6A). This dolostone deposited in the initial phase of transgression (Wendte & Uyeno 2005), as shown by considerable depletion of $\delta^{13}C$ signatures (Fig. 14), indicating precipitation in the conditions of mixing marine and meteoric waters (Immenhauser et al. 2003; Kirmaci 2008; Kozlowski & Munnecke 2010). Type 1 dolomite was obviously formed in shallow-marine periphery of marine basins during early diagenesis. Due to low porosity and high density of the rock, the dolomite crystals mainly preserved the initial characteristics and were little affected by later diagenetic events.

The relatively good preservation of fabric, fine crystal size and dull cathodoluminescence response of type 2 dolomite of the Upper Pskov unit suggest rapid replacement of marine lime mud by dolostone during an early stage of diagenesis in shallow marine subtidal and supratidal environments. The lamination of the rock (Figs 3C, 6B) is similar to precipitation of platform interior environments separated from open sea (Flügel 2004). Due to high porosity later diagenetic fluids have overprinted the initial deposit. Some voids are rimmed with Mn-rich tiny crystals (Figs 7, 10) that have precipitated from later diagenetic fluids. Later, obviously after uplift of the territory, part of the voids became rimmed or occluded with authigenic calcite crystals due to the action of circulating mixed marine/freshwater karst-related fluids. In some places pigmentation with iron oxides appeared (Figs 6B, 7). The freshwater-enriched fluids affected also the whole rock composition, causing lower $\delta^{18}O$ and $\delta^{13}C$ values (Fig. 14B).

The formation of non-stoichiometric scattered concentric zoned dolomite rhombs of type 3 in limestone matrix (Figs 6C, 8, 9) represents the initial phase of dolomitization (Török 2000; Fig. 15). Growth of individual dolomite crystals requires nucleation sites and constant supply of the dolomitizing fluid. It is possible that the nuclei were more widely spaced during the first phase of dolomitization, which resulted in only partial dolomitization of limestone (Jones 2005). The centre of the dolomite crystal around the nucleation site contains microcrystalline dolomite and calcite grains (Fig. 9), representing relict material derived from locally replaced carbonate mud during the initial phase of crystal formation, while the clear rim forms by continuing growth during diagenesis (Daniel & Haggerty 1988; Amthor & Friedman 1991; Machel 2004; Rameil 2008). The formation of concentric zoned dolomite crystals is believed to associate with dolomitizing fluids of temporally variable composition at the site of dolomite crystals growth (Kyser et al. 2002; Jones 2005; Carmichael et al. 2008). Such dolomite crystals have been interpreted as being of shallow burial mixing-zone origin (Dix 1993). Voids inside the zoned crystals are produced by dissolution of calcium-rich particles (Jones 2005; Fig. 8C). Cores of dolomite crystals may have dissolved during late diagenesis (Kyser et al. 2002; Kirmaci & Akdag 2005). Dark cortices observed in cathodoluminescence (Fig. 8B) suggest redistribution of

Table 4. Carbon and oxygen isotope data of void-filling carbonate and host rock

Unit	Section	Depth, m	Matrix	Dolomite type	Void filling	$\delta^{18}O$, ‰	$\delta^{13}C$, ‰
Upper Pskov	Tsiistre	48.3	Dolostone	4		−4.77	0.99
	Tsiistre	48.3			Dolomite	−4.85	0.91
	Tsiistre	49.6	Dolostone	4		−4.93	−0.9
	Tsiistre	49.6			Dolomite	−4.64	−0.74
	Tsiistre	50.5	Dolostone	4		−4.17	−0.25
	Tsiistre	50.5			Dolomite	−5.07	−1.00
	Ape	1.4	Dolostone	4		−5.38	0.48
	Ape	1.4			Dolomite	−5.39	0.42
	Ape	2.8	Dolostone	2		−5.31	0.06
	Ape	2.8			Dolomite	−5.55	−0.11
	Marinova 5		Dolostone	4		−5.52	0.46
	Marinova 5				Dolomite	−5.28	−0.15
	Marinova 2		Dolostone	4		−6.38	−0.52
	Marinova 2				Dolomite	−5.26	−0.91
	Marinova 1A		Dolostone	4		−7.54	−1.01
	Marinova 1A				Calcite	−11.97	−1.93
	Marinova 1		Dolostone	4		−3.42	−1.63
	Marinova 1				Calcite	−6.46	−5.20
	Marinova 4		Limestone			−4.86	−1.65
	Marinova 4				Calcite	−7.9	−2.22
	Marinova 3		Limestone			−11.65	−2.05
	Marinova 3				Calcite	−12.25	−1.96

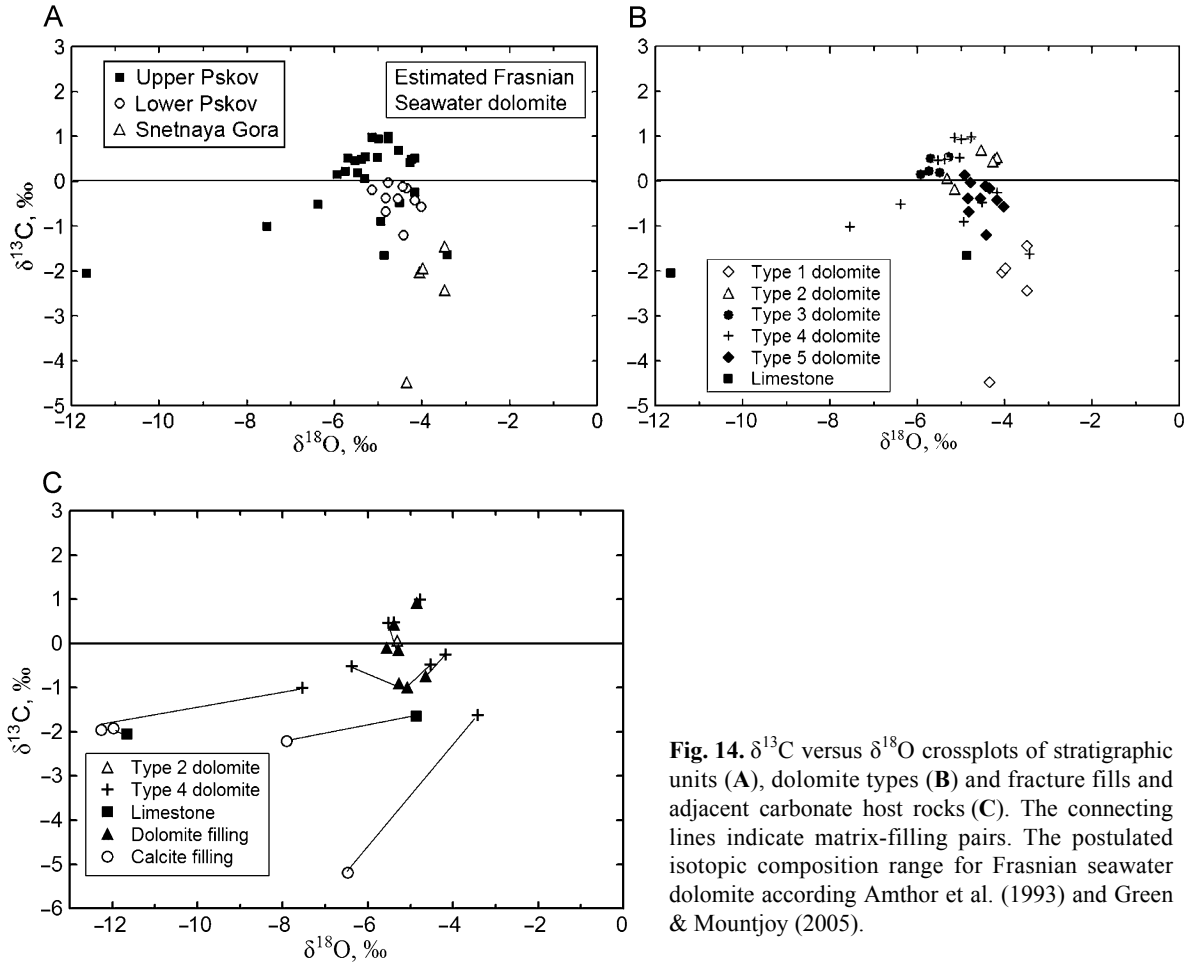

Fig. 14. $\delta^{13}C$ versus $\delta^{18}O$ crossplots of stratigraphic units (**A**), dolomite types (**B**) and fracture fills and adjacent carbonate host rocks (**C**). The connecting lines indicate matrix-filling pairs. The postulated isotopic composition range for Frasnian seawater dolomite according Amthor et al. (1993) and Green & Mountjoy (2005).

Diagenetic event	Diagenesis stages Early Late
Mechanical compaction	·····
Type 1 dolomite	·····
Type 2 dolomite	·····
Fracturing, creation of porosity	·····
Type 3 dolomite	·····
Sucrosic dolomite, type 4	····· ···· ·····
Corrosion of dolomite rhombs	·····
Type 5 dolomite	·····
Type 6 dolomite	·····
Karstification	·····
Influx of Mn-containing fluids	·····
Precipitation of illite	·····
Void-filling dolomite	·····
Dedolomitization	·····
Void-filling calcite	·····

Fig. 15. Suggested paragenetic sequence of the Plavinas rocks in the study area.

material by circulation of pore fluids after the grain boundary configuration was attained (Yardley & Lloyd 1989). Curtailing the dolomitizing fluid would, possibly, stop the dolomitization process (Jones 2005). Hereby the matrix is remained as fossil-rich unaltered micritic limestone (Figs 6C, 8A). Concentric zoned dolomite crystals occur in the Upper Pskov unit, in the uppermost part of an upwards shallowing lagoonal/peritidal incompletely dolomitized sequence (Fig. 2, Table 2).

Sucrosic dolomites, typical of the Upper Pskov unit (Figs 3D, 6D, 10, Table 2), are distinguished as type 4 dolomites, which have a complicated diagenetic history. According to Choquette et al. (1992), such dolomites are formed during shallow burial dolomitization in peritidal to subtidal conditions. Judging from planar crystal faces (Figs 6D, 10A), dolomite precipitation occurred at low temperatures (<50 °C; Lumsden & Caudle 2001; Jones 2005). After the first phase of dolomitization the formed voids were saturated with marine-like pore waters, which circulated along conduits and through dissolution and precipitation might have formed transparent outer rims chemically similar to cores. However, the features of corrosion of the dolomite crystal core point to a possibility that some time interval remained between the formation of the inner crystal and growth of cortices (Figs 6D, 10A; Amthor & Friedman 1992; Choquette & Hiatt 2008). In the following phase of diagenesis, the influx of Mn-rich fluids caused precipitation of tiny crystals on the walls of voids, revealed by bright red cathodoluminescence light. Besides voids the stylolites served as conduits for these fluids (Fig. 10B). This process was preceded by the occlusion of the voids. Void-filling dolomite crystals are chemically similar to matrix dolomite, but exhibit a coarser crystal size and transparency (Fig. 13). According to stable isotope signatures, dolomite fills lay in the same field with sucrosic dolomites and their signatures only slightly differ from each other (Fig. 14C, Table 4). However, dolomite fillings and also dolostones containing fillings and fractures show $\delta^{13}C$ values depleted up to −1‰ compared to host sucrosic dolomites (Fig. 14B). Obviously, fluids that formed during the late stage of diagenesis altered the matrix of sucrosic dolomite and obliterated its previous characteristics. The same phenomenon is known also from other studies (Swart et al. 2005). Most probably, yellowish-brown authigenic fillings between zoned crystals, which according to EDS study contain Al, Si, K and Fe pointing to illite composition, are also products of late diagenesis (Figs 10D, 15; Kleesment 2007). The changes in clay minerals may provide the source of manganese in burial conditions (Tucker & Wright 1990). Some of the voids are filled with calcite (Fig. 7, Table 4). The calcite-filling event clearly postdates the above-described episodes (Figs 14C, 15).

Fine- to medium-crystalline compact dolostone (Fig. 3B) containing type 5 dolomite (Figs 6E, 11A) occurs commonly in the Lower Pskov unit (Table 2). Type 5 dolomite is interpreted to be formed during early diagenesis in subtidal to peritidal settings by rapid dolomitization of lime mud postdating early submarine cementation (Amthor & Friedman 1992; Özkan & Elmas 2009). Open voids without younger fills (Fig. 11A) point to the absence of the influence of later fluids. Negative values of $\delta^{13}C$ indicate mixing marine and freshwater conditions (Immenhauser et al. 2003). Obviously, dolomitization took place at the final stage of the transgression.

Slightly porous compact Ca-rich dolostone containing inequigranular non-stoichiometric dolomite of type 6 (Figs 6F, 12) occurs as rare interbeds in the boundary beds of the Lower and Upper Pskov units and in the Hino section of the Upper Pskov unit. Its character suggests a long-lasting dolomitization event (Özkan & Elmas 2009). In all likelihood, the dolomite crystals grew slowly, thereby preserving textural details, and eventually joined along compromise boundaries (Fig. 6F). It is possible that type 6 dolomite is partly recrystallized from type 2 and type 5 dolomites. Recrystallization could be affected by calcite-rich waters, causing an increase in the Ca/Mg ratio (Bates et al. 2008). The inferred slow crystal growth requires a long residence time of the rocks to be in contact with the dolomitizing solutions in stable hydrologic conditions (Amthor & Friedman 1992). The Fe-rich level in dolomite crystals (Figs 6F, 12A) was most probably formed by precipitation of Fe-oxides after leaching out of Ca-rich particles (Nader et al. 2007), possibly during late diagenesis in the deep subsurface (Mountjoy et al.

1999). However, the non-stoichiometric composition of such crystals remains unclear.

After pervasive lithification and dolomitization of subtidal and supratidal facies deposits the studied rocks were subjected to subaerial erosion during uplift and emergence of the basin at the end of the Frasnian Age. Surface and shallow subsurface karstification processes, which have repeatedly been reported (Paukstys & Narbutas 1996; Satkunas et al. 2007), developed in the rocks of Pskov and Chudovo ages during the Late Frasnian up to the present.

Deep-discharge of meteoric fluids during the periods of karstification in the overlying strata is the source of undersaturated fluids causing dolomite dissolution and necessary porosity and conduits for pore water circulation, as well as freshwater invasion into the sequence (Bishoff et al. 1994; Cunningham et al. 2009). Dissolution of precursor dolomite may also provide a source of Ca^{2+} for late diagenetic calcite fillings and dedolomitization processes. Dolomite calcitization (dedolomitization) has been associated with sulphate dissolution (Fu et al. 2006; Nader et al. 2008; Rameil 2008). Late diagenetic calcite precipitation and dedolomitization in Devonian rocks of southeastern Estonia have obviously been related to influx of gypsum-bearing vadose fluids. Dissolution of gypsum led to overcharge of fluids with Ca^{2+} ions, resulting in the dissolution of dolomite and precipitation of calcite along the flow path of percolating fluids. East- and southwards of the investigated area gypsum-bearing deposits are distributed in the overlying Upper Devonian Dubnik section (Sorokin 1978; Kajak 1997), which may be the origin of these fluids. Circulation of the fluids has proceeded horizontally along layers affecting the Upper Pskov level in the studied sequence.

Some voids are occluded with calcite fillings (Fig. 7); in some interlayers calcitization of dolomite has taken place (Fig. 4B). The originally pervasively dolomitized rocks show calcitization through dissolution/precipitation. During dedolomitization, Mg, Al, K, Fe and Na were released from the precursor dolomite into the solution. The precipitating calcite does not incorporate these elements (Nader et al. 2008) and, therefore, the content of insoluble residue is abnormally low (<0.7%).

With regard to stable isotope values, dedolomite and calcite fillings differ essentially between samples, from each other and from the matrix rock. Large differences exist between adjacent host rock and fracture fillings (Fig. 14C, Table 4), whose isotope values correspond to karst-related precipitations (Török 2000; Nader et al. 2008). According to the great variability in stable isotope values, it is possible that the fillings originate from different stages of karstification processes. It has been suggested that dedolomitization and remagnetization proceeded simultaneously and often were coeval with orogenetic processes (Nick & Elmore 1990; Zegers et al. 2003). In the northern part of the Baltic basin two remagnetization events accompanying karst features have been distinguished: the Late Devonian–Carboniferous and Late Jurassic–Early Cretaceous episodes (Katinas & Nawrocki 2004; Plado et al. 2008). The most negative values of $\delta^{18}O$ (below –11‰; Fig. 14C, Table 4) might reflect higher temperatures and/or fluids associated with later Hercynian orogenetic compression events (Wright et al. 2004) and suggest penecontemporaneous formation of dedolomitic rock in Marinova quarry (sample 3) with its void-filling calcite and calcite fill of sample 1A (Fig. 14C, Table 4). The dedolomitic rock of Marinova sample 4 with its void-filling calcite and calcite fill of dolomite sample 1 belong to some other event. Dedolomitization and calcite-filling processes took place during late diagenesis (Fig. 15).

CONCLUSIONS

Based on petrographic, mineralogical and geochemical data of the Frasnian sequence of southern Estonia and northern Latvia, the following conclusions were made.

1. Carbonate rocks of the Plavinas RS were affected by multistage diagenetic events. Great differences in stable isotope signatures of the dolostones/dolomites and dolomites precipitated from Frasnian seawater point to extensive postdepositional alterations. Later processes have largely overprinted the earlier formed rocks. On the basis of crystal characteristics, six different dolomite textures were identified.
2. According to $\delta^{18}O$ and $\delta^{13}C$ values, low Mn and Fe contents, dull luminescent colour of crystals and dominant planar character of crystal boundaries, the dolomites were mainly formed at relatively low temperatures (<50 °C).
3. Dolomitization is more pronounced in the lower part of the studied sequence. Carbonates of the Snetnaya Gora Fm and the Lower Pskov unit are completely dolomitized, whereas those of the Upper Pskov unit and Chudovo Fm are partially dolomitized and contain interbeds of calcareous dolomites and limestones. Decrease in the dolomite content in the upper part of the section suggests the upward percolation of dolomitizing fluids.
4. Stable isotope results indicate that during the transgressive phase of deposition (Snetnaya Gora Fm and Lower Pskov unit), dolomitizing fluids were represented by a mixture of meteoric and sea water.
5. Highly porous rocks with void-filling authigenic phases of dolomite or calcite are depleted in $\delta^{18}O$ and $\delta^{13}C$ values. Void-filling processes have also affected the rock matrix.

6. Late diagenetic karst-related processes have greatly affected the rocks of the Plavinas RS. A major dedolomitization and calcite-filling phase occurred as a result of migration of karst-related meteoric waters into previously dolomitized horizons within the Frasnian carbonate rocks during the final uplift and emergence of the northern part of the Baltic basin.

Acknowledgements. The study was supported by the Estonian Research Council (projects SF0320080s07, SF0140016s09 and grant 8182). Special thanks are due to Rein Sinisalu for the opportunity to describe and sample the Ape drill core and to Ain Põldvere for providing unpublished drill core data from southeastern Estonia (both from the Geological Survey of Estonia). The authors are grateful to Gennadi Baranov for help with figures and photography. The paper greatly benefited from constructive reviews by Jüri Plado and Girts Stinkulis.

REFERENCES

Amthor, J. E. & Friedman, G. M. 1991. Dolomite-rock textures and secondary porosity development in Ellenburger Group carbonates (Lower Ordovician), west Texas and southeastern New Mexico. *Sedimentology*, **38**, 343–362.

Amthor, J. E. & Friedman, G. M. 1992. Early- to late-diagenetic dolomitization of platform carbonates: Lower Ordovician Ellenburger Group, Permian basin, West Texas. *Journal of Sedimentary Research*, **62**, 131–144.

Amthor, J. E., Mountjoy, E. W. & Machel, H. G. 1993. Subsurface dolomites in Upper Devonian Leduc build-ups, central part of Rimbey-Medowbrook reef trend, Alberta, Canada. *Bulletin of Canadian Petroleum Geology*, **41**, 164–185.

Azmy, K., Knight, I., Lavoie, D. & Chi, G. 2009. Origin of dolomites in the Beat Harbour Formation, St. George Group, in western Newfoundland, Canada: implications for porosity development. *Bulletin of Canadian Petroleum Geology*, **57**, 81–104.

Bates, G. S., Kendall, A. C. & Millar, L. L. 2008. Determining the origin of karst fill at the Sub-Mesozoic uncorformity, southeastern Saskatchewan. In *Summary of Investigations 2008*, **1**, Saskatchewan Geological Survey, Paper A-6, 9 pp. [CD-ROM].

Bishoff, J. L., Ramon, J., Shanks, W. C. & Rosenbauer, R. J. 1994. Karstification without carbonic acid; bedrock dissolution by gypsum-driven dedolomitization. *Geology*, **22**, 995–998.

Buggisch, W. & Joachimski, M. M. 2006. Carbon isotope stratigraphy of the Devonian of Central and Southern Europe. *Palaeogeography, Palaeoclimatology, Palaeoecology*, **240**, 68–88.

Buggisch, W. & Mann, U. 2004. Carbon isotope stratigraphy of Lochkovian to Eifelian limestones from the Devonian of central and southern Europe. *International Journal of Earth Sciences*, **93**, 521–541.

Carmichael, S. K., Ferry, J. M. & McDonough, W. F. 2008. Formation of replacement dolomite in the Latemar carbonate buidup, Dolomites, northern Italy: Part I. Field relations, mineralogy, and geochemistry. *American Journal of Science*, **308**, 851–884.

Choquette, P. W. & Hiatt, E. E. 2008. Shallow-burial dolomite cement: a major component of many ancient sucrosic dolomites. *Sedimentology*, **55**, 423–460.

Choquette, P. W., Cox, A. & Meyers, W. J. 1992. Characteristics, distribution and origin of porosity in shelf dolostones: Burlington-Keokuk Formation (Mississippian), U.S. mid-continent. *Journal of Sedimentary Petrology*, **62**, 167–189.

Cioppa, M. T., Al-Aasm, I. S., Symons, D. T. A. & Gillen, K. P. 2003. Dating penecontemporaneous dolomitization in carbonate reservoirs: paleomagnetic, petrographic, and geochemical constraints. *AAPG Bulletin*, **87**, 71–88.

Coniglio, M., Zheng, Q. & Carter, T. R. 2003. Dolomitization and recrystallization of middle Silurian reefs and platformal carbonates of the Guelph Formation, Michigan Basin, southwestern Ontario. *Bulletin of Canadian Petroleum Geology*, **51**, 177–199.

Cunningham, K. J., Sukop, M. C., Huang, H., Alvarez, P. F., Curran, H. A., Renken, R. A. & Dixon, J. F. 2009. Prominence of ichnologically influenced macroporosity in the karst Biscayne aquifer: stratiform "super-K" zones. *GSA Bulletin*, **121**, 164–180.

Daniel, M. M. & Haggerty, J. A. 1988. Diagenesis of the Upper Jurassic–Lower Cretaceous carbonate platform of the Galicia margin at ocean drilling program site 639. *Proceedings of the Ocean Drilling Program, Scientific Results*, **103**, 155–169.

Dix, G. R. 1993. Patterns of burial and tectonically controlled dolomitization in an Upper Devonian fringing-reef complex: Leduc Formation, Peace River arch area, Alberta, Canada. *Journal of Sedimentary Petrology*, **63**, 628–640.

Drivet, E. & Mountjoy, E. W. 1997. Dolomitization of the Leduc Formation (Upper Devonian), southern Rimbey-Meadowbrook Reef Trend, Alberta. *Journal of Sedimentary Research*, **67**, 411–423.

Flügel, E. 2004. *Microfacies of Carbonate Rocks*. Springer-Verlag, Berlin, Heidelberg, 976 pp.

Fu, Q., Qing, H. & Bergman, K. M. 2006. Dolomitization of the Middle Devonian Winnipegosis carbonates in south-central Saskatchewan, Canada. *Sedimentology*, **53**, 825–848.

Green, D. G. & Mountjoy, E. W. 2005. Fault and conduit controlled burial dolomitization of the Devonian west-central Alberta Deep Basin. *Bulletin of Canadian Petroleum Geology*, **53**, 101–129.

Hardie, L. A. 1987. Dolomitization: a critical view of some current views. *Journal of Sedimentary Petrology*, **57**, 166–187.

Immenhauser, A., Porta, G. D., Kenter, J. A. M. & Bahamonde, J. R. 2003. An alternative model for positive shifts in shallow-marine carbonate $\delta^{13}C$ and $\delta^{18}O$. *Sedimentology*, **50**, 953–959.

Jones, B. 2005. Dolomite crystal architecture: genetic implications for the origin of the Tertiary dolostones of the Cayman Islands. *Journal of Sedimentary Research*, **75**, 177–189.

Kajak, K. 1997. Upper Devonian. In *Geology and Mineral Resources of Estonia* (Raukas, A. & Teedumäe, A., eds), pp. 121–123. Estonian Academy Publishers, Tallinn.

Kallaste, T. & Kiipli, T. 1995. Discrete dolomite phases in carbonate rocks: results of the mathematical treatment of

X-ray diffraction peaks. *Proceedings of the Estonian Academy of Sciences, Geology*, **44**, 211–220.

Katinas, V. & Nawrocki, J. 2004. Mesozoic remagnetization of Upper Devonian carbonates from the Česis and Skaistgirys quarries (Baltic states). *Geological Quarterly*, **48**, 293–298.

Kirmaci, M. Z. 2008. Dolomitization of the late Cretaceous–Paleocene platform carbonates, Gölköy (Ordu), eastern Pontides, NE Turkey. *Sedimentary Geology*, **203**, 289–306.

Kirmaci, M. Z. & Akdag, K. 2005. Origin of dolomite in the Late Cretaceous–Paleocene limestone turbidites, Eastern Pontides, Turkey. *Sedimentary Geology*, **181**, 39–57.

Kleesment, A. 2007. Devonian. In *Tsiistre (327) Drill Core* (Põldvere, A., ed.), *Estonian Geological Sections*, 8, 10–19.

Kleesment, A. & Shogenova, A. 2005. Lithology and evolution of Devonian carbonate and carbonate-cemented rocks in Estonia. *Proceedings of the Estonian Academy of Sciences, Geology*, **54**, 153–180.

Kleesment, A., Kirsimäe, K., Martma, T., Shogenova, A., Urtson, K. & Shogenov, K. 2012. Linkage of diagenesis to depositional environments and stratigraphy in the northern part of the Baltic basin. *Estonian Journal of Earth Sciences*, **61**, 15–32.

Kozlowski, W. & Munnecke, A. 2010. Stable carbon isotope development and sea-level changes during the Ludlow (Silurian) of the Lysogóry region (Rzepin section, Holy Cross Mountains, Poland). *Facies*, **56**, 615–633.

Kyser, T. K., James, N. P. & Bone, Y. 2002. Shallow burial dolomitization and dedolomitization of Cenozoic cool-water limestones, Southern Australia: geochemistry and origin. *Journal of Sedimentary Research*, **72**, 146–157.

Lavoie, D., Chi, G., Brennan-Alpert, P., Desrochers, A. & Bertrand, R. 2005. Hydrothermal dolomitization in the Lower Ordovician Romaine Formation of the Anticosti Basin: significance for hydrocarbon exploration. *Bulletin of Canadian Petroleum Geology*, **53**, 454–472.

Lonnee, J. & Al-Aasm, I. 2000. Dolomitization and fluid evolution in the Middle Devonian Sulphur Point Formation, Rainbow South Field, Alberta: petrographic and geochemical evidence. *Bulletin of Canadian Petroleum Geology*, **48**, 262–283.

Luczaj, J. A., Harrison III, W. B. & Williams, N. S. 2006. Fractured hydrothermal dolomite reservoirs in the Devonian Dundee Formation of the central Michigan Basin. *AAPG Bulletin*, **90**, 1787–1801.

Lumsden, D. N. & Caudle, G. C. 2001. Origin of massive dolostone: the Upper Knox model. *Journal of Sedimentary Research*, **71**, 400–409.

Machel, H. G. 2004. Concept and models of dolomitization: a critical reappraisal. *Geological Society London, Special Publications*, **235**, 7–63.

Machel, H. G. & Buschkuehle, B. E. 2008. Diagenesis of the Devonian Southesk-Cairn carbonate complex, Alberta, Canada: marine cementation, burial dolomitization, thermochemical sulphate reduction, anhydritization, and squeegee fluid flow. *Journal of Sedimentary Research*, **78**, 366–389.

Machel, H. G. & Mountjoy, E. W. 1986. Chemistry and environments of dolomitization – a reappraisal. *Earth Science Reviews*, **23**, 175–222.

Maliva, R. G., Budd, D. A., Clayton, E. A., Missimer, T. M. & Dickson, J. A. D. 2011. Insights into the dolomitization process and porosity modification in sucrosic dolostones, Avon Park Formation (Middle Eocene), East-Central Florida, U.S.A. *Journal of Sedimentary Research*, **81**, 218–232.

Mark-Kurik, E. & Põldvere, A. 2012, Devonian stratigraphy in Estonia: current state and problems. *Estonian Journal of Earth Sciences*, **61**, 33–47.

Mazzullo, S. J. 1994. Dolomitization of periplatform carbonates (Lower Permian, Leonardian), Midland basin, Texas. *Carbonates and Evaporites*, **9**, 95–112.

Mountjoy, E. W., Machel, H. G., Green, D., Duggan, J. & Williams-Jones, A. E. 1999. Devonian matrix dolomites and deep burial carbonate cements: a comparison between the Rimbey-Meadowbrook reef trend and the deep basin of west-central Alberta. *Bulletin of Canadian Petroleum Geology*, **47**, 487–509.

Nader, F. H., Swennen, R. & Ellam, R. M. 2007. Field geometry, petrography and geochemistry of a dolomitization front (Late Jurassic, central Lebanon). *Sedimentology*, **54**, 1093–1119.

Nader, F. H., Swennen, R. & Keppens, E. 2008. Calcitization/dedolomitization of Jurassic dolostones (Lebanon): results from petrographic and sequential geochemical analyses. S*edimentology*, **55**, 1467–1485.

Nick, K. E. & Elmore, R. D. 1990. Paleomagnetism of the Cambrian Royer dolomite and Pennsylvanian Collings Ranch conglomerate, southern Oklahoma: an early Paleozoic magnetization and nonpervasive remagnetization by weathering. *Geological Society of America Bulletin*, **102**, 1517–1525.

Nikishin, A. M., Ziegler, P. A., Stephenson, R. A., Cloetingh, S. A. P. L., Furne, A. V., Fokin, P. A., Ershov, A. V., Bolotov, S. N., Korotaev, M. V., Alekseev, A. S., Gorbachev, V. I., Shipilov, E. V., Lankreijer, A., Bembinova, E. Y. U. & Shalimov, I. V. 1996. Late Precambrian to Triassic history of the East European Craton: dynamics of sedimentary basin evolution. *Tectonophysics*, **268**, 23–63.

Özkan, A. M. & Elmas, A. 2009. Petrographic characteristic of the Kiziloren Formation (Upper Triassic–Lower Jurassic) in the Acpinar (Konya–Turkey) area. *Ozean Journal of Applied Sciences*, **2**, 451–464.

Paukstys, B. & Narbutas, V. 1996. Gypsum karst of the Baltic Republics. *International Journal of Speleology*, **25**, 279–284.

Plado, J., Preeden, U., Puura, V., Pesonen, L. J., Kirsimäe, K. & Elbra, T. 2008. Palaeomagnetic age of remagnetifications in Silurian dolomites, Rõstla quarry (Central Estonia). *Geological Quarterly*, **52**, 213–224.

Põldvere, A. (ed.). 2007. Tsiistre (327) drill core. *Estonian Geological Sections*, 8, 1–56.

Põldvere, A. 2012. Kagu-Eesti karbonaatne Devon pakub geoloogile üllatusi [Carbonate Devonian rocks of Southeast Estonia offer surprises to geologists]. *Eesti Geoloogiakeskuse Toimetised*, **11**, 69–77 [in Estonian].

Potma, K., Weissenberger, J. A. W., Wong, P. K. & Gilhooly, M. G. 2001. Toward a sequence stratigraphic framework for the Frasnian of the Western Canada Basin. *Bulletin of Canadian Petroleum Geology*, **49**, 37–85.

Qing, H. 1998. Petrography and geochemistry of early-stage, fine- and medium-crystalline dolomites in the Middle Devonian Presqu'ile Barrier at Pine Point, Canada. *Sedimentology*, **45**, 433–446.

Rameil, N. 2008. Early diagenetic dolomitization and dedolomitization of Late Jurassic and earliest Cretaceous platform

carbonates: a case study from the Jura Mountains (NW Switzerland, E France). *Sedimentary Geology*, **212**, 70–85.

Read, J. F. 1985. Carbonate platform facies models. *AAPG Bulletin*, **69**, 1–21.

Rifai, R. I., Kolkas, M. M., Holail, H. M. & Khaled, K. A. 2006. Diagenesis and chemistry of the Aptian dolomite (Cretaceous) in the Razzak oil field, Western desert, Egypt. *Carbonates and Evaporites*, **21**, 176–187.

Satkunas, J., Marcinkevicius, V., Mikulenas, V. & Taminskas, J. 2007. Rapid development of karst landscape in North Lithuania – monitoring of denudation rate, site investigations and implications for management. *GFF*, **129**, 345–350.

Shogenova, A., Shogenov, K., Pesonen, L. J. & Donadini, F. 2007. Chemical composition and physical properties of the rock. In *Tsiistre (327) Drill Core* (Põldvere, A., ed.), *Estonian Geological Sections*, 8, 21–29, Appendices 1, 8, 9.

Sibley, D. F. & Gregg, J. M. 1987. Classification of dolomite rock texture. *Journal of Sedimentary Petrology*, **57**, 967–975.

Sorokin, V. S. 1978. *Étapy razvitiya severo-zapada Russkoj platformy vo franskom veke* [*Evolutionary Stages of the Russian Platform During the Frasnian Age*]. Zinatne, Riga, 282 pp. [in Russian].

Stinkulis, G. 1998. *Transitional Zones of Siliciclastic–Carbonate Rocks and Limestones–Dolostones in Devonian of Latvia*. Summary of the dissertation for the Doctoral Degree in Geology, University of Latvia, Riga, 60 pp.

Stinkulis, G. 2008. Kapec devona kalkameni Latvija tagad ir dolomite? [Why is the Devonian limestone in Latvia today dolomite?]. *Geografija Geologija Vides Zinatne: Referatu tezes, Riga, LU*, **66**, 14–16 [in Latvian].

Suuroja, K. 1997. *The Bedrock Geological Map of Estonia. Scale 1 : 400 000. Explanatory Note*. Unpublished report of the Geological Survey of Estonia, Tallinn, 60 pp.

Swart, P. K., Cantrell, D. L., Westphal, H., Handford, C. R. & Kendall, C. G. 2005. Origin of dolomite in the Arab-D reservoir from the Ghawar field, Saudi Arabia: evidence from petrographic and geochemical constraints. *Journal of Sedimentary Research*, **75**, 476–491.

Tänavsuu-Milkeviciene, K., Plink-Björklund, P., Kirsimäe, K. & Ainsaar, L. 2009. Coeval versus reciprocal mixed carbonate-siliciclastic deposition, Middle Devonian Baltic Basin, Eastern Europe: implications from the regional tectonic development *Sedimentology*, **56**, 1250–1274.

Török, A. 2000. Formation of dolomite mottling in Middle Triassic ramp carbonates (Southern Hungary). *Sedimentary Geology*, **131**, 131–145.

Tucker, M. E. & Wright, V. P. 1990. *Carbonate Sedimentology*. Blackwell Scientific Publication, Oxford, 482 pp.

Van Geldern, R., Joachimski, M. M., Day, J., Jansen, U., Alvarez, F., Yolkin, E. A. & Ma, X.-P. 2006. Carbon, oxygen and strontium isotope records of Devonian shell calcite. *Palaeogeography, Palaeoclimatology, Palaeoecology*, **240**, 47–67.

Vandeginste, V., Swennen, R., Gleeson, S. A., Ellam, R. M., Osadetz, K. & Roure, F. 2009. Thermochemical sulphate reduction in the Upper Devonian Cairn Formation of the Fairholme carbonate complex (South-West Alberta, Canadian Rockies): evidence from fluid inclusions and isotopic data. *Sedimentology*, **56**, 439–460.

Warren, J. 2000. Dolomite: occurrence, evolution and economically important associations. *Earth Science Reviews*, **52**, 1–81.

Wendte, J. & Uyeno, T. 2005. Sequence stratigraphy and evolution of Middle to Upper Devonian Beaverhill Lake strata, south-central Alberta. *Bulletin of Canadian Petroleum Geology*, **53**, 250–354.

Wright, W. R., Sommerville, I. D., Gregg, J. M., Shelton, K. L. & Johnson, A. W. 2004. Irish Lower Carboniferous replacement dolomite: isotopic modelling evidence for a diagenetic origin involving low-temperature modified seawater. *Geological Society, London, Special Publications*, **235**, 75–97.

Yardley, B. W. D. & Lloyd, G. E. 1989. An application of cathodoluminescence microscopy to the study of textures and reactions in high-grade marbles from Connemara, Ireland. *Geological Magazine*, **126**, 333–337.

Zegers, T. E., Dekkers, M. J. & Bailly, S. 2003. Late Carboniferous remagnetization of Devonian limestones in the Ardennes: role of temperature, fluids, and deformation. *Journal of Geophysical Research*, **108**, B7, 2357.

Ülem-Devoni Plavinase lademe dolokivide petrograafia ja koosseisu evolutsioon Eesti lõuna- ning Läti põhjaosas

Anne Kleesment, Kristjan Urtson, Tarmo Kiipli, Tõnu Martma, Anne Põldvere, Toivo Kallaste, Alla Shogenova ja Kazbulat Shogenov

Ülem-Devoni Plavinase lademe läbilõige Balti basseini põhjaosas on esindatud domeriidi ja lubjakivi vahekihte sisaldavate dolokividega. Dolokivide uuringud polarisatsiooni-, katoodluminestsentsi- ja eletronmikroskoobis ning kivimite süsiniku ja hapniku isotoopide suhted viitavad kivimite keerukale diageneetilisele evolutsioonile. Petrograafiliste ja geokeemiliste andmete alusel eraldati kuus erinevat dolomiidi tüüpi. Valdavalt on tegemist stöhhiomeetrilise koosseisu ja väikese raua- ning mangaanisisaldusega dolomiitidega. Isotoopkoostise alusel erinevad dolomiidid selgelt Frasne mereveest settinud dolomiitidest. Dolomitisatsioon on tugevam uuritava läbilõike alumises osas. Snetnaja Gora ja Pskovi kihistu karbonaadid on täielikult dolomitiseerunud, läbilõike ülemises osas on see protsess olnud mittetäielik. Pskovi kihistu alumises osas on dolokivi poorid valdavalt avatud, läbilõike ülemises osas on aga tühemikud diageneesi käigus osaliselt või täielikult täitunud hilisemate kristallidega. Täidiseks olevate dolomiidikristallide isotoopkoostis erineb emakivimi omast mõnevõrra, kaltsiitse täidise puhul on aga isotoopkoosseisu erinevus märkimisväärne. Settimisjärgselt on kivimid olnud pikka aega subaeraalses keskkonnas, mille vältel on need allunud karstistumisprotsesside mõjule.